AD A092727

LEVEL II

(12)

B.S.

SGI-R-80-021

RELATIVE RECEIVER FUNCTIONS FOR THREE DIFFERENT ARRAY CONCEPTS

G. M. LUNDQUIST
G. R. MELLMAN
D. M. HADLEY

DTIC
ELECTE
DEC 10 1980
S D
E

SEMI-ANNUAL TECHNICAL REPORT
FOR PERIOD DECEMBER 1,1977 - MAY 31, 1980

SPONSORED BY
ARPA ORDER No. 2551

This research was supported by the Advanced Research Projects Agency of the Department of Defense and was monitored by AFTAC/VSC, Patrick AFB, FL. 32925, under Contract No. F08606-79-C-0009.

The views and conclusions contained in this document are those of the authors and should not be interpreted as necessarily representing the official policies, either expressed or implied, of the Advanced Research Projects Agency, The Air Force Technical Applications Center, or the United States Government.

July 1, 1980

Approved for Public Release, Distribution Unlimited

DDC FILE COPY

SIERRA GEOPHYSICS, INC.
150 N. SANTA ANITA AVENUE • ARCADIA, CALIFORNIA 91006 • (213) 574-7052

393821

80 12 05 041

APTAC Project Authorization: VT/0710

ARPA Order: 2551

Effective Date of Contract: November 22, 1978

Contract Expiration Date: September 30, 1980

Contract No: F08606-79-C-0009

Principal Investigator and Phone No.:

Dr. Robert S. Hart

(213) 574-7052

Program Manager and Phone No:

Mr. Michael J. Shore

(202) 325-7581

Sierra Geophysics, Inc.

150 N. Santa Anita Ave. • Suite 880 • Arcadia, California 91006 • (213) 574-7052

SGI-R-80-021

RELATIVE RECEIVER FUNCTIONS FOR THREE DIFFERENT ARRAY CONCEPTS

G. M. LUNDQUIST

G. R. MELLMAN

D. M. HADLEY

SEMI-ANNUAL TECHNICAL REPORT

FOR PERIOD DECEMBER 1,1977 - MAY 31, 1980

SPONSORED BY

ARPA ORDER No. 2551

This research was supported by the Advanced Research Projects Agency of the Department of Defense and was monitored by AFTAC/VSC, Patrick AFB, FL. 32925, under Contract No. F08606-79-C-0009.

The views and conclusions contained in this document are those of the authors and should not be interpreted as necessarily representing the official policies, either expressed or implied, of the Advanced Research Projects Agency, The Air Force Technical Applications Center, or the United States Government.

July 1, 1980

Approved for Public Release, Distribution Unlimited

SECURITY CLASSIFICATION OF THIS RAGE (When Data Entered)

REPORT DOCUMENTATION PAGE

READ INSTRUCTIONS BEFORE COMPLETING FORM

1. REPORT NUMBER

2. GOVT ACCESSION NO. AD-A092727

3. RECIPIENT'S CATALOG NUMBER

4. TITLE (and Subtitle)
(6) Relative Receiver Functions for Three Different Array Concepts.

5. TYPE OF REPORT & PERIOD COVERED
Semi-Annual Technical Report 12/1/77-5/31/80

6. PERFORMING ORG. REPORT NUMBER
(14) SGI-R-80-021

7. AUTHOR(s)
(10) G. M./Lundquist, G. R./Mellman, and D. M./Hadley

8. CONTRACT OR GRANT NUMBER(s)
(15) Contract No. F08606-79-C-0009

9. PERFORMING ORGANIZATION NAME AND ADDRESS
Sierra Geophysics, Inc.
150 No. Santa Anita Ave.
Arcadia, CA 91006

10. PROGRAM ELEMENT, PROJECT, TASK AREA & WORK UNIT NUMBERS
ARPA Order ~~No.~~ 2551

11. CONTROLLING OFFICE NAME AND ADDRESS
AFTAC/VSC
Patrick AFB, FL 32925

12. REPORT DATE
July 1, 1980

13. NUMBER OF PAGES
45

14. MONITORING AGENCY NAME & ADDRESS(if different from Controlling Office)
(9) Semi-Annual Technical rept. 1 Dec 77 - 31 May 80,

15. SECURITY CLASS. (of this report)
Unclassified

15a. DECLASSIFICATION/DOWNGRADING SCHEDULE

16. DISTRIBUTION STATEMENT (of this Report)
Approved for Public Release, Distribution Unlimited
(11) 1 Jul 80

17. DISTRIBUTION STATEMENT (of the abstract entered in Block 20, if different from Report)
(12) 51

18. SUPPLEMENTARY NOTES

19. KEY WORDS (Continue on reverse side if necessary and identify by block number)
Receiver Functions
Deconvolution
Body Waves

20. ABSTRACT (Continue on reverse side if necessary and identify by block number)
This technical report summarizes work done during the period December 1979 - May 1980 on the computation of relative receiver functions. Such functions are vitally important to the understanding of explosion or earthquake source functions, since the effects of crustal reverberations, local amplification effects and lateral variations in attenuation near seismic stations cannot otherwise be separated from source or source crustal properties. Two steps are involved in the calculation. Trace deconvolutions

DD FORM 1 JAN 73 1473

393 821

SECURITY CLASSIFICATION OF THIS PAGE (When Data Entered)

#20 continued

generated by spectral ratios are averaged in the log-spectral domain. Then the relative receiver functions are computed for all stations in an array by use of a non-linear recursive technique. The result is a filter which may be used to model near receiver contributions to synthetic seismograms of stations in the array.

Results are presented for three different array concepts, including a small array of a few kilometer aperture, an array made up of all of the WWSSN stations in the western U.S., and an array made up of all SRO stations in a usable distance range about the Eastern Kasakh test site. In each case, the methods are applied successfully, with the primary limitations being data availability.

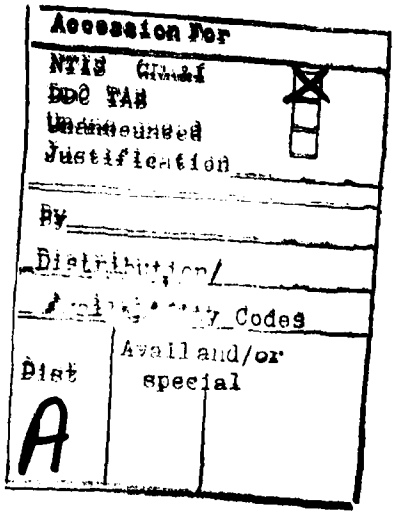

TABLE OF CONTENTS

I. INTRODUCTION

The object of this study is to produce a function, R, for a given station which models all near-receiver contributions to observed waveforms, including crustal reverberations, acoustic impedance amplification effects, laterally-refracted arrivals, and variations (δt^*) in attenuation from an average earth model. Clearly R must be a function of back azimuth to the source and incidence angle for any but the simplest receiver region structures. Thus R must be re-evaluated for each source region under consideration.

As a first step toward a true receiver function, we have computed relative receiver functions, RRF's, for three types of arrays. The method uses spectral ratios to isolate the near receiver part of the total propagation filter. What is actually obtained is the ratio, R_s/R_o, of the response of a secondary station to the response at a reference station. Because any (frequency dependent) factor common to both stations will divide out, we obtain only r_s/r_o, the ratio of relative receiver functions. Resolution of the absolute individual receiver responses, R_o and R_s will require careful calibration of the reference station.

From an array of stations, we can compute $d_j = r_j/r_o$, from which we may synthesize the seismogram at station j using the seismogram at the reference station. The final step is to recover r_o, and thus r_j; so that we may compute the synthetic seismogram at station j, j = 0, 1, ...n, using theoretical

sources. The recovery of r_o from the d_j requires the imposition of an additional constraint, and we have chosen to require the $r_j(t)$ to be as simple or "delta-like" as possible. The technique used for this simplicity criterion is known as Minimum Entropy Deconvolution, or MED (Wiggins, 1978).

The total procedure has been applied with varying amounts of success to three different array concepts. The first is the Yucca Flats array of maximum dimension about 4 km. The second "array" is the "Western U.S. Array," or WUSA, made up of all of the WWSSN stations west of about 105° W longitude in the United States. The third array concept is that of a global array which includes any seismograph or array of seismometers in the distance range $30\text{-}90^{\circ}$ from an explosion source region. Clearly, each array concept is different; hence the results will be discussed separately.

II. TECHNICAL DISCUSSION

2.1 Trace Deconvolution

Success in obtaining relative receiver functions requires that the near-receiver response be isolated. In general this is done by dividing a reference trace spectrum of the form

$$t_o(\omega) = S(\omega,\theta,h)\cdot C_s(\omega,\theta,i,h)\cdot G(\omega,\Delta)\cdot Q(\omega,\Delta)\cdot C_R(\omega,\theta,e)\cdot I(\omega) \quad (1)$$

into a secondary trace spectrum of the same form. In equation (1), S is the source spectrum; C_s and C_R are source and receiver crustal responses; G is geometric spreading; Q represents the anelastic attenuation and I is the instrument. Functional dependencies are on frequency, ω, the azimuth, θ, incidence angles i and e at source and receiver, respectively, and source depth, h.

If the two stations in the deconvolution are close, then all terms except C_R in the ratio of forms like (1) will divide out, independent of source type or teleseismic path length. (Deconvolution of the instruments may be handled separately if necessary.) This type of deconvolution was done successfully by Hart et al. (1979) for the YF and OB arrays at NTS. In that study, the variance of individual estimates of each deconvolved trace

$$d_j = \frac{t_j}{t_o} \quad (2)$$

was reduced using a log-spectral stack, and the resulting average transfer functions between the reference and various secondary stations could be used to interpret lateral variations in geology across the sedimentary basin beneath Yucca Flats.

If the stations in the array are not proximate, then more care must be taken in the choice of sources and paths. In order to get sources at a common back azimuth from stations in the Western U.S. Array, earthquake sources were used from South America (southeastern azimuth) and the Aleutian-Kurile-Japan arc (northwestern azimuth). The sampling of focal mechanism diagrams from the southeast azimuth shown in Figure 1 demonstrates that, even though the array is continental in size, the rays sample only a very small part of the focal mechanism. If care is taken to avoid nodal lines, then the source term in (1) will divide out.

By the same arguments, the source crustal response cannot change much when the azimuth changes by less than 15^{o} and the ray parameter changes by less than .02 sec/km. The variation which does exist within these limits will be additive noise in the deconvolution traces. Insofar as that noise is incoherent from trace to trace, it will be minimized by the log-spectral stack and the MED process.

If care is taken to avoid caustics, the geometric attenuation filter is frequency independent and reduces to a simple gain factor. In the work done here, each trace is corrected to a common distance so that $G(\Delta)$ divides out during deconvolution.

The Q filter is a more difficult problem because the upper mantle may not be the same beneath all stations. The Q filter may be written in the form

$$e^{-\frac{\omega}{2}(t^*+\delta t^*)} \qquad (3)$$

LOWER HEMISPHERE

P ARRIVALS

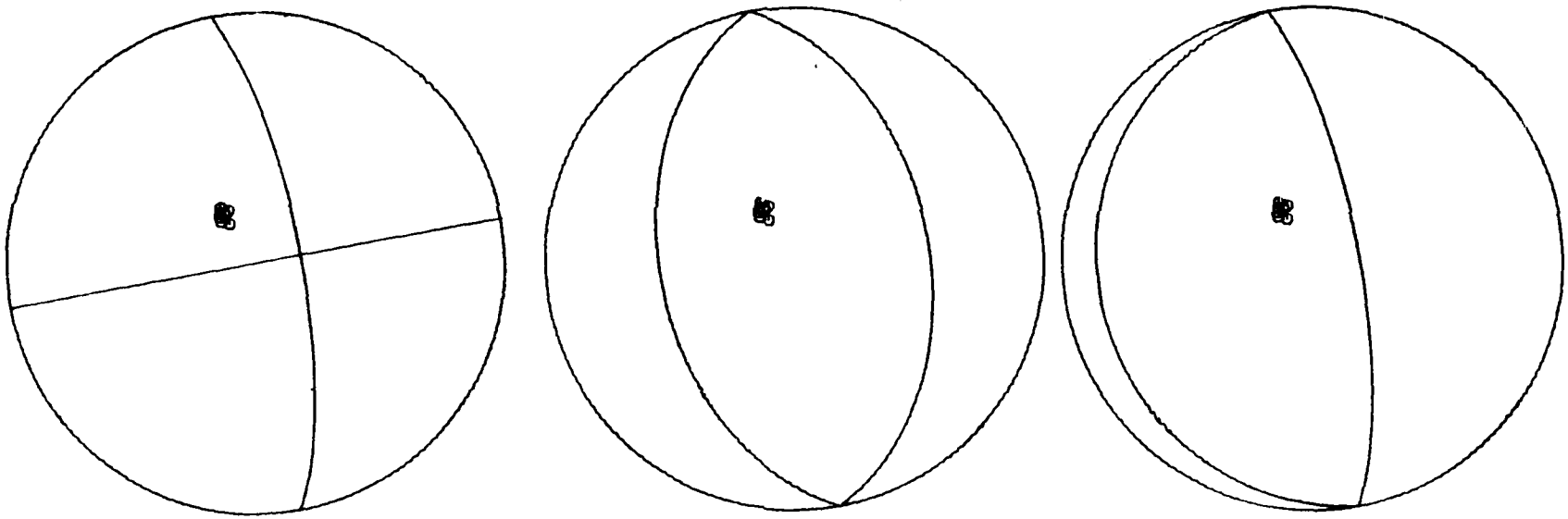

STRIKE	350	350	350
DIP	75	45	75
RAKE	0	90	90

Figure 1. Sample focal mechanisms from a South American earthquake zone to demonstrate the size of the Western U.S. Array.

where t* is the complex anelastic attenuation operator for an average earth, and δt^* represents the variation from average. Fortunately, there is good evidence that t* is nearly constant with distance for $30° < \Delta < 90°$ (Mellman and Hart, 1980). Even when a frequency dependent Q is considered, Lundquist (1979) showed that $t^*(\omega)$ is expected to be nearly constant with distance for any frequency. Thus the first factor in (3) will divide out during deconvolution, leaving

$$e^{-\frac{\omega}{2}(\delta t_i^* - \delta t_o^*)} \qquad (4)$$

This factor will remain in the receiver function to represent the difference in anelastic attenuation in the crust and upper mantle beneath the two stations. In many applications, such as yield estimation or m_b, this relative δt^* measure will be a very desirable part of the receiver function.

An example of the deconvolution of two traces with significantly different δt^* is shown in Figure 2. If the low frequency (large δt^*) trace is used for the reference trace, then (4) becomes a rising exponential and the deconvolution becomes unstable (third trace). Thus it is reasonable to choose the station with the highest apparent frequency content to be the reference station, because the difference in Q filters will tend to stabilize the deconvolution (fourth trace).

To extend this procedure from continental arrays using sources over narrow azimuths to global arrays using stations at any azimuth about a confined source region requires the use of explosion data to minimize asymmetries of the source. There

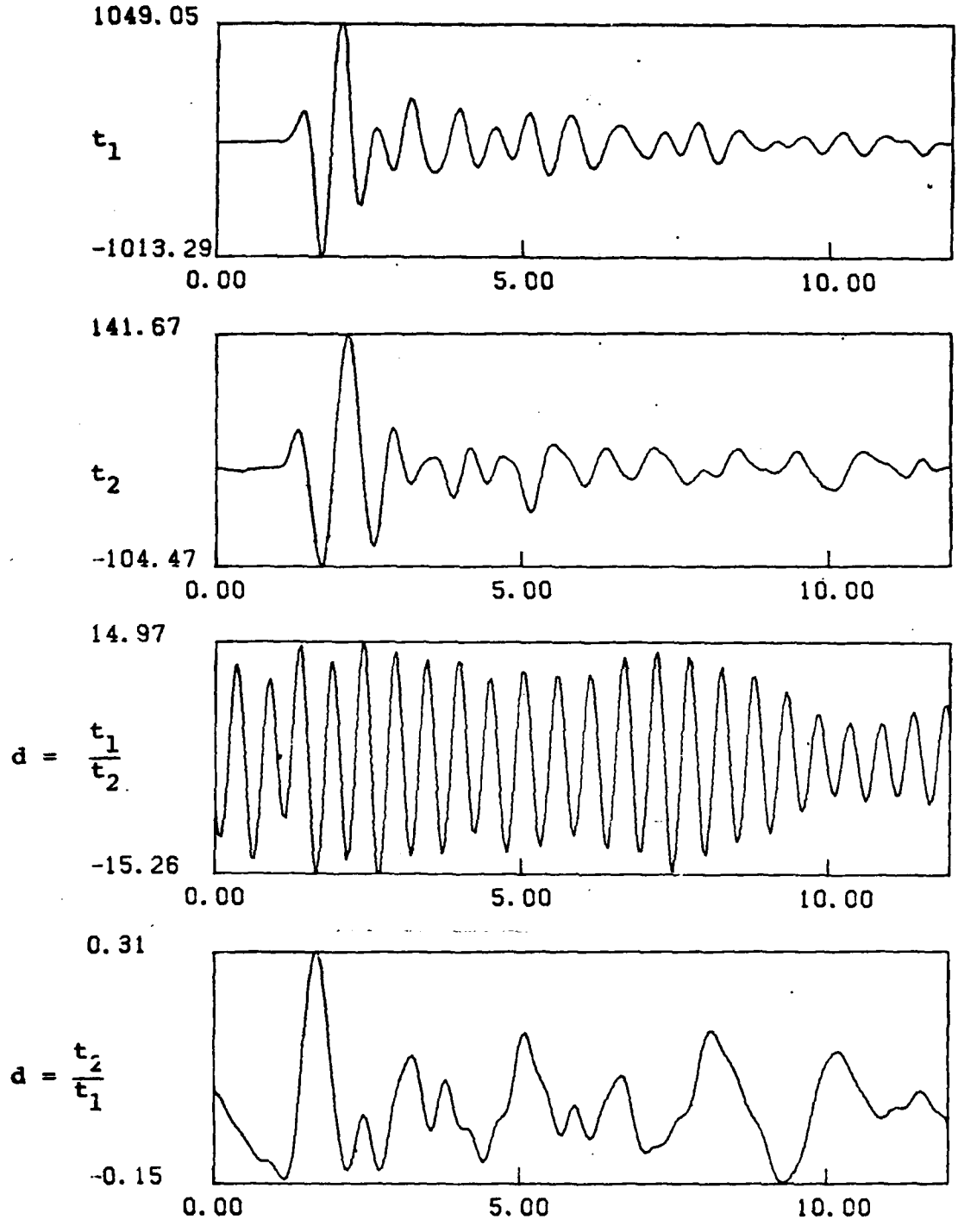

Figure 2. Sample deconvolution trace pair with obvious δt^*. Division by the low frequency spectrum gives an inverse Q filter; while division by the high frequency spectrum gives a stable deconvolution.

will almost certainly be residual source crust factors, δC_s, even with the absence of focal mechanism and directivity effects. Thus it is more important than before to average over several events for noise reduction. Any consistent azimuthal variation in the source radiation cannot be distinguished from a receiver effect; so the best average will include sources in different geologies and different structures of any given test site. Once receiver functions are determined, of course, then asymmetric source radiation may be studied at the stations of the global array.

In summary, the differences between deconvolution for the different array types may be visualized in terms of the log spectral domain.

$$D_k(\omega,\theta,i) = \frac{1}{n}\sum_j \log d_{kj} = \underbrace{\frac{1}{n}\sum_j \log\left(\frac{C_{R_k}}{C_{R_o}}\right)_j}_{\text{small array}} \underbrace{-\frac{\omega}{2}(\delta t_k^* - \delta t_o)_j}_{\text{continental array}} \underbrace{+\log\left(\frac{\delta C_{S_k}}{\delta C_{S_o}}\right)_j}_{\text{global array}} \qquad (5)$$

In each case, relaxation of constraints on spatial dimension of the array adds potential complexity to the receiver function. Of course microseismic and recording system noise form an additive term to each type.

2.2 Minimum Entropy Deconvolution

Trace deconvolution provides n pieces of information, $d_i = r_i/r_o$, about the n+1 unknown receiver functions $r_o, r_i, \ldots r_n$.

In order to recover r_o and thus the r_j, Hart et al. (1979) adapted the Minimum Entropy Deconvolution technique (Wiggins, 1978). The process attempts to find a linear operator which, when convolved with each trace in the set, maximizes the order (or minimizes the entropy) of the set as a whole. The new constraint on the problem is thus to find r_o such that all of the receiver functions are as simple or "delta-like" as possible.

A useful measure of simplicity (Wiggins, 1978) is the weighted varimax norm.

$$V = \sum_j w_j v_j = \sum_j w_j \frac{\int r_j^4(t)dt}{(\int r_j^2(t)dt)^2} \tag{6}$$

Hart et al. (1979) showed that maximization of V in the frequency domain is equivalent to solving the system of non-linear simultaneous equations.

$$\hat{f}_o^*(\omega) = \frac{\sum_j \frac{w_j}{u_j^2} \hat{f}_j^3(\omega)\, d_j^*(\omega)}{\sum_j \frac{v_j w_j}{u_j} d_j^*(\omega)\, d_j(\omega)} \tag{7}$$

where (^) implies an estimated value as opposed to a known value, and (*) implies complex conjugate. In that $d_j = r_j/r_o$, then $\hat{f}_j = \hat{f}_o d_j$; and $u_j = \int \hat{f}_j(t)dt$ is simply the energy in each filtered trace. In general, the first guess for $\hat{f}_o$ is a delayed delta function, $\delta(t-t_o)$, and three to five iterations through (7) will determine a local maximum in variance (minimum in entropy).

A few observations on (7) may be made. First, note that the denominator is a weighted sum of power spectra; so the division tends to emphasize low amplitude spectral content and flatten the spectrum of r_o. Second, the numerator is a cross spectral product between a given trace and the cube of the estimated receiver function. This is equivalent to shaping the spectrum to that of a time domain function made up of a few large spikes.

Under most configurations, the MED process converges to a maximum of the varimax norm, but the position of the maximum varies with choice of reference station, choice of weight functions and use of causal truncations. In that the filter is initialized as a spike, the most reasonable, and, indeed, generally most successful, choice for reference station is the simplest and highest frequency station. The primary importance of the weight functions is to prevent MED from reaching a spike configuration for any r_j. Thus, the reference station is generally underweighted by w= .01 and other simple stations by smaller amounts.

The effect of MED processing is to take a set of n relatively complex trace deconvolutions and output n+1 receiver functions. Note again that any factor common to all of the stations in the array will have been lost during the processing; so that the r_j are still relative receiver functions in that they cannot predict absolute amplitude. Calibration of one station in the array, however, will permit calculations of absolute amplitudes for all stations.

2.3 Estimated Relative Receiver Functions

In this section results will be presented for both trace deconvolution and FMED processing for each of the array concepts. The small array data have been presented earlier by Hart et al. (1979) and are only briefly reviewed here.

2.3.1 YF and OB Arrays at NTS

Figure 3 is an example of the input data and the quality of the trace deconvolution for a study done on the SDCS stations at Yucca Flats, NTS. The traces on the left are the reference traces from station OB2NV located at Climax Stock. The dashed line traces at the right are the secondary station data, in this case, station YF2NV. The solid line traces are reconvolutions of the reference trace with the average deconvolved signal shown at the bottom. That is,

$$\hat{e}_i = t_o d_i$$

where (^) again implies estimated or synthesized quantity. It is quite clear that the trace deconvolutions stack well enough to predict the seismogram at the secondary station. The implication is that the deconvolution has indeed isolated receiver effects from the other path effects.

Figure 4 shows the estimated RRF's for the 5 stations in this test. Note that station OB2 on granite has a much simpler response than the YF stations located on a sedimentary basin. The effect of the more complex responses is demonstrated in Figure 5 in which the RRF's have been convolved with a typical explosion source-time function. Although the source term tends

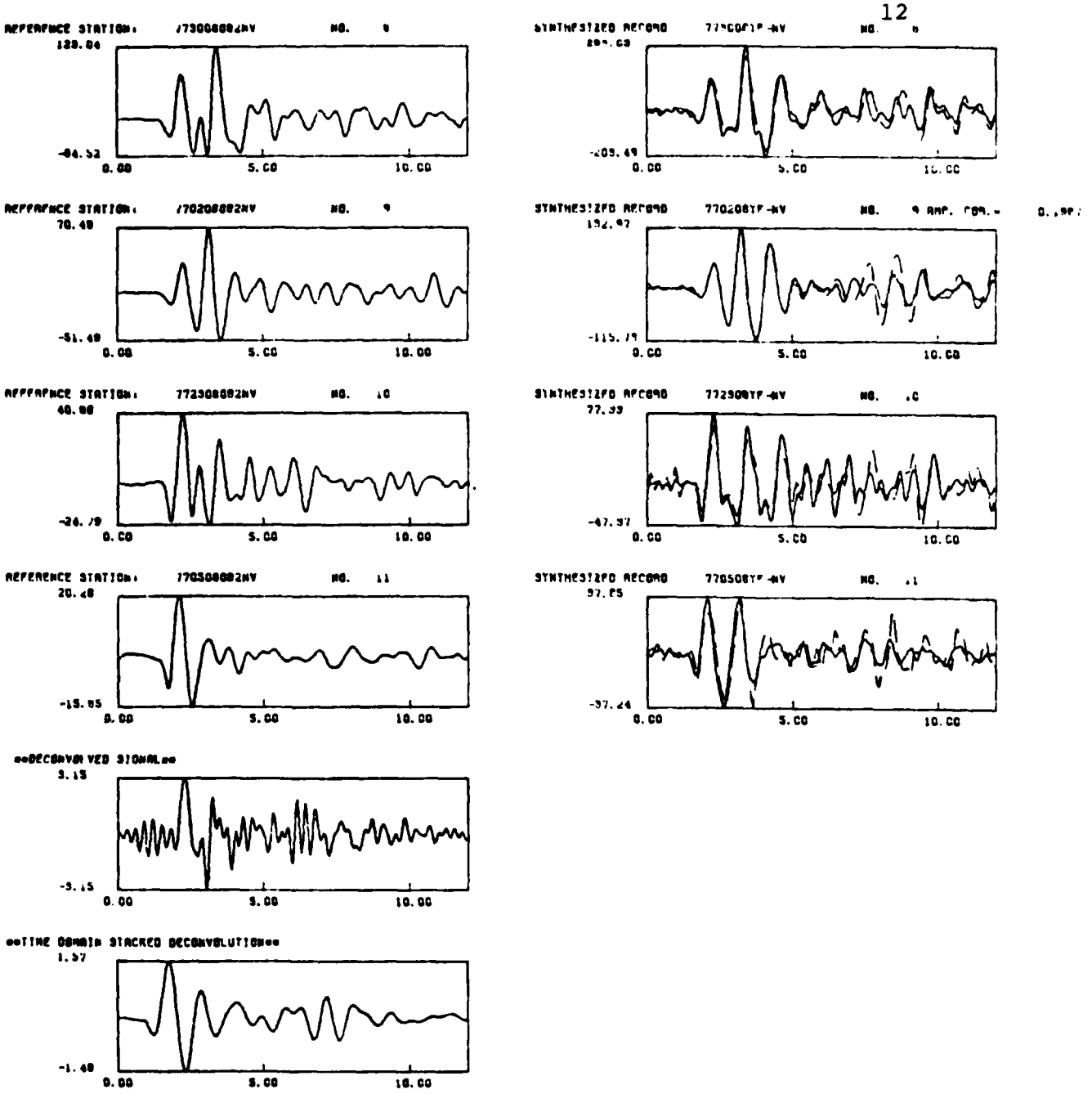

Figure 3. Observed seismograms at stations OB2NV (left) and YF2NV (right, dashed) from events to the southeast. Synthetic seismograms (right, solid) for station YF2NV produced by convolving the OB2NV observation with the YF2 receiver functions appropriate to a southeast azimuth.

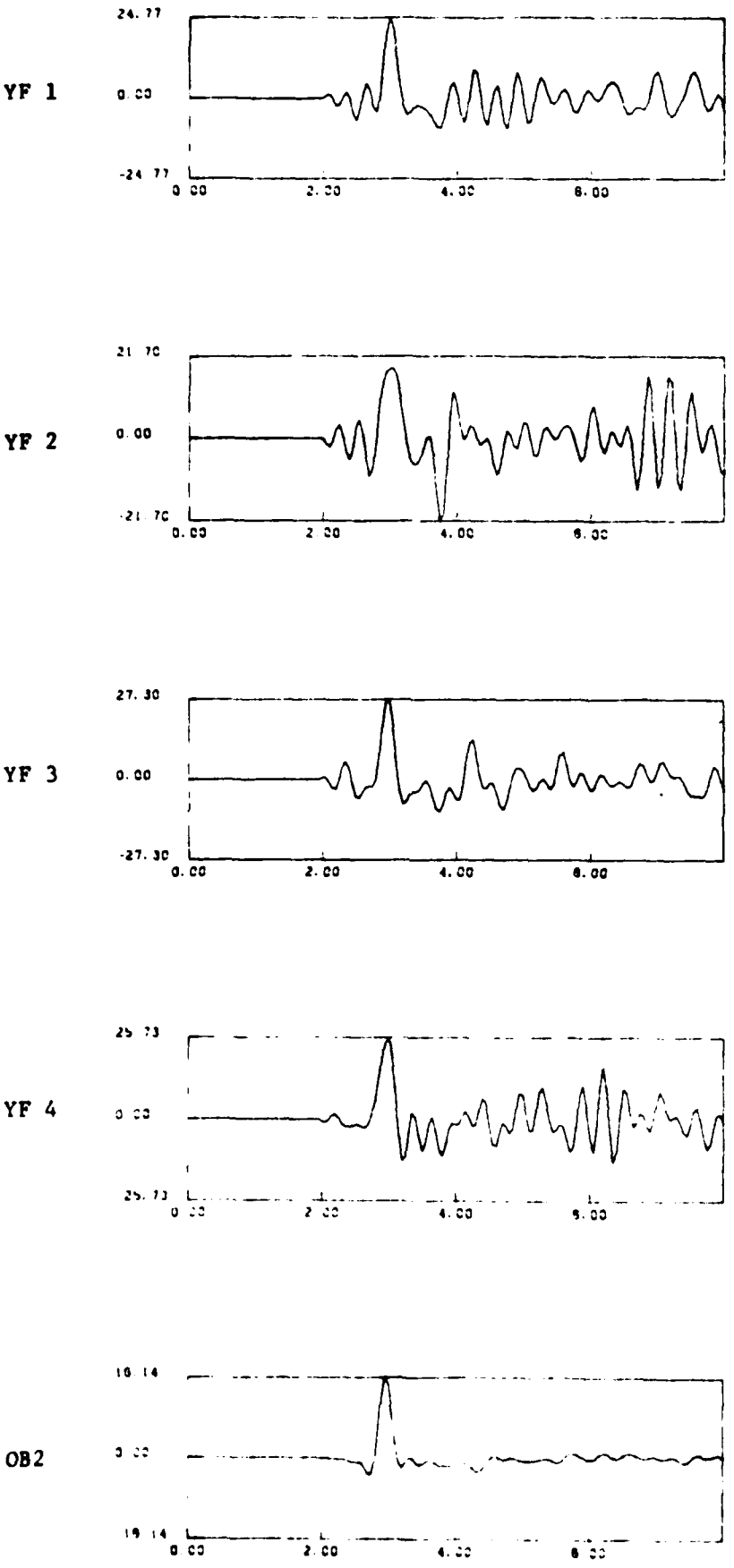

Figure 4. Receiver functions for the 4 YF array stations and the station OB2 appropriate to a southeast azimuth.

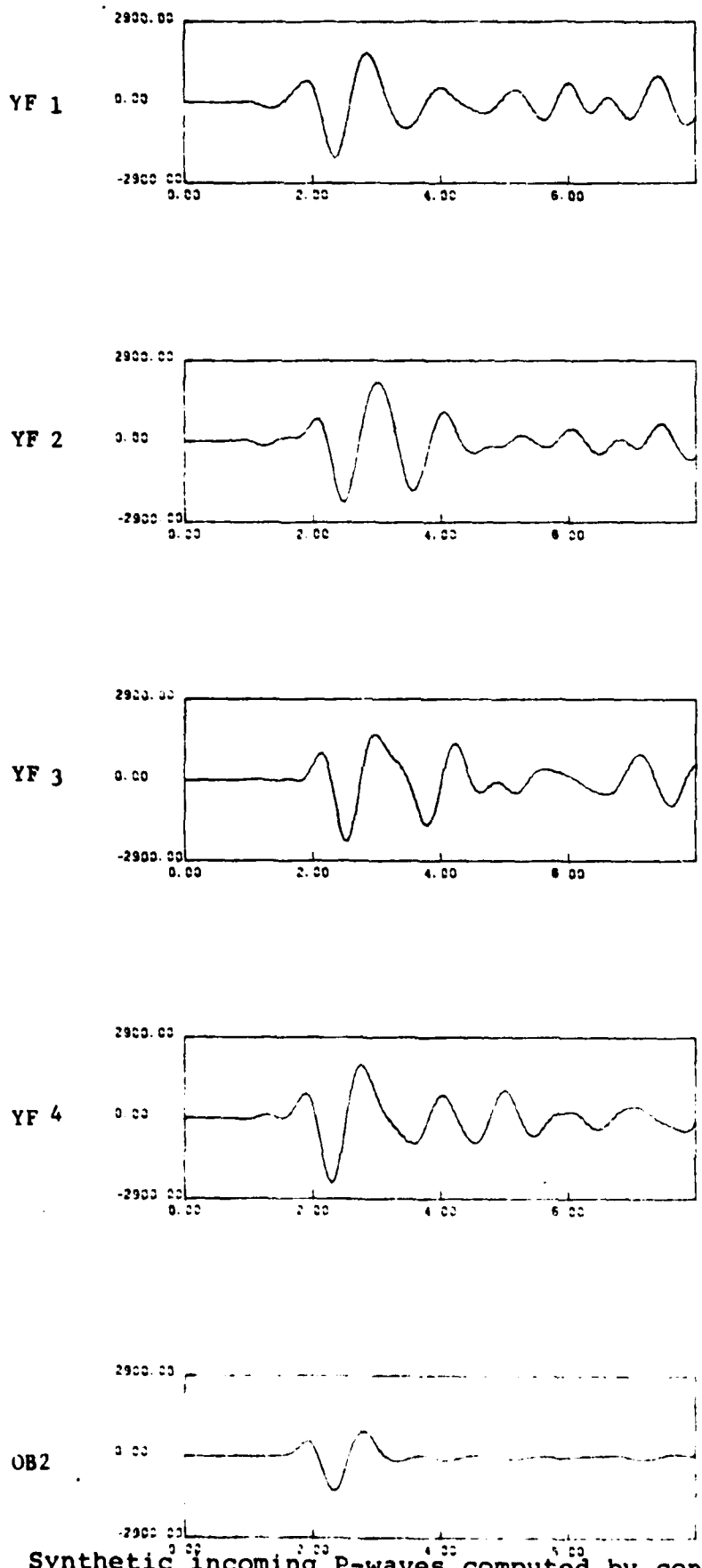

Figure 5. Synthetic incoming P-waves computed by convolving the receiver functions shown in Figure 4 (southeast azimuth) with an explosion source.

to smooth out the details in each RRF, some distortion of the main arrival may be seen, and later arrivals are received in the sedimentary basin that do not appear in the granite stock.

Perhaps the most significant result relates to amplitude measurements such as m_b. The RRF's predict that signals seen through the sediments will have up to twice the amplitude of signals seen through the igneous stock. Note that the same relative amplification would be predicted if the acoustic impedance in both rock types were varied by any common factor, demonstrating again why these receiver responses must be considered relative to each other.

2.3.2 Western United States Array

The stations in the Western U.S. Array, or WUSA are shown relative to their geologic province in Figure 6. All of the WWSSN stations west of the Rocky Mountain front were considered, but MSO and BOZ were excluded due to insufficient data for the events used. This left an 8 station array of maximum aperture of about 18^{o}, representing a variety of geologic and tectonic settings. Station TUC was used as the reference station for trace deconvolution both because of its quality and the simple fact that it had more usable records than any of the other station.

The events used for computation of RRF's from a southeastern azimuth are listed in Table 1. These events were carefully selected for consistency in first motion across the array, and events with obviously complex source time functions were omitted. Also given is the data availability. The number of traces in the log spectral averages varied from 4 to 7.

Figures 7 to 13 show the results of the trace deconvolutions. The data are arranged in pairs, with the reference trace on top

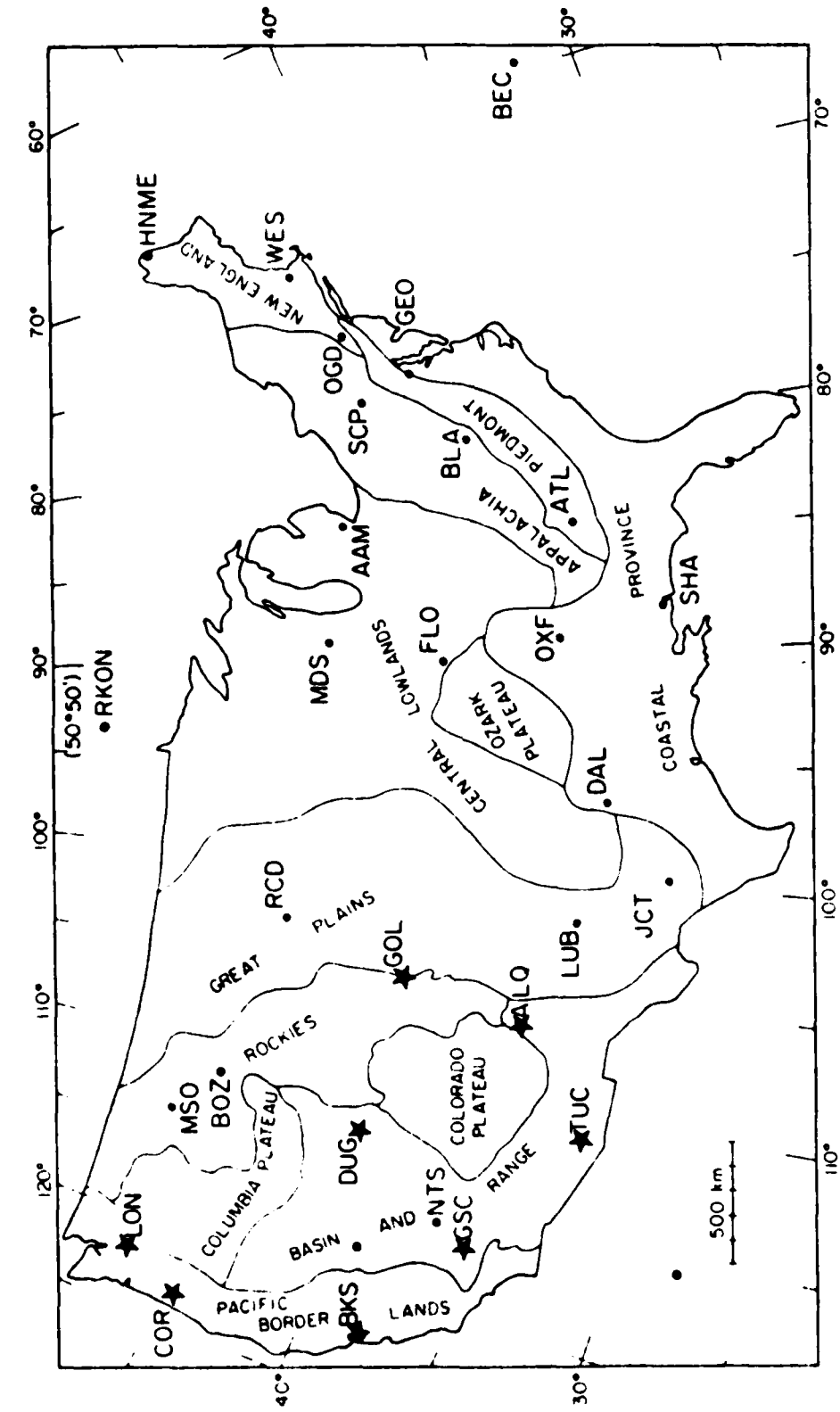

Figure 6. Locations of WWSSN and SDCS stations in the United States relative to approximate physiographic provinces. The Western U.S. Array stations are marked with stars.

TABLE 1. SOUTH AMERICAN EVENT LIST

DATE	TIME	LOCATION		ALQ	BKS	COR	DUG	GOL	GSC	LON	TUC
4/25/67	10:26:14	32.6S	69.0W	X	X		X	X		X	X
11/15/67	21:35:51	28.7S	71.2W	X	X	X		X		X	X
2/6/68	11:19:23	28.5S	71.0W	X	X	X		X	X	X	X
4/21/68	9:23:35	23.4S	70.5W	X							X
4/30/68	23:51:18	38.4S	71.1W		X		X		X	X	X
9/30/76	8:04:11	24.2S	68.2W		X	X	X		X	X	X
12/3/76	5:37:34	21.0S	69.0W	X	X		X	X	X		X
3/13/77	4:55:55	2.0S	58.0W				X		X		X
6/8/77	13:25:16	22.1S	67.3W		X	X			X		X

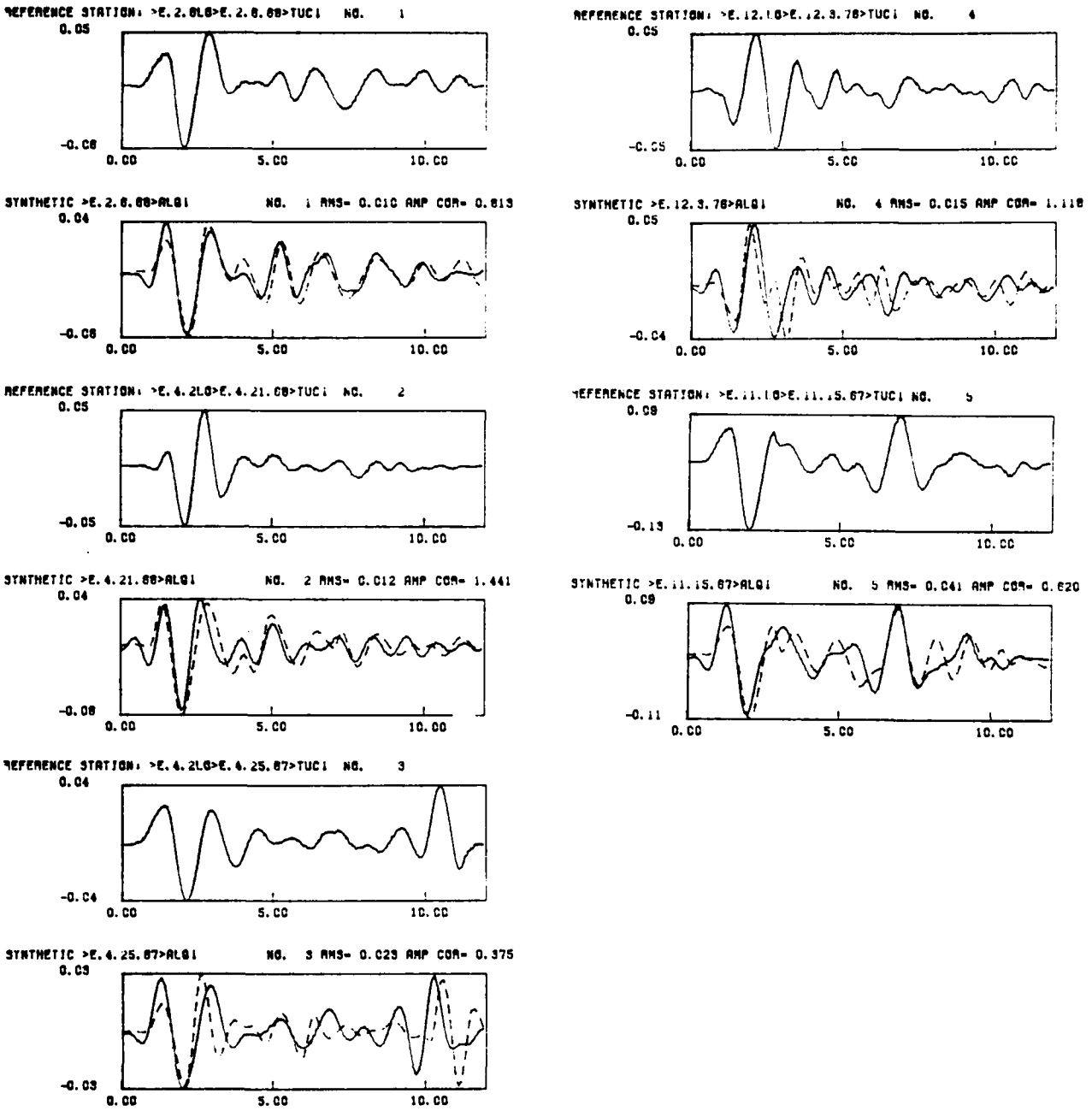

Figure 7. Data and synthetic for the station pair ALQ/TUC for events from a southeastern azimuth. For each trace pair, the reference trace is plotted above, and the secondary trace (dashed line) is plotted below. Synthetic seismograms (solid line below) are produced by convolving the TUC observation with the log-spectral average of ALQ/TUC deconvolutions.

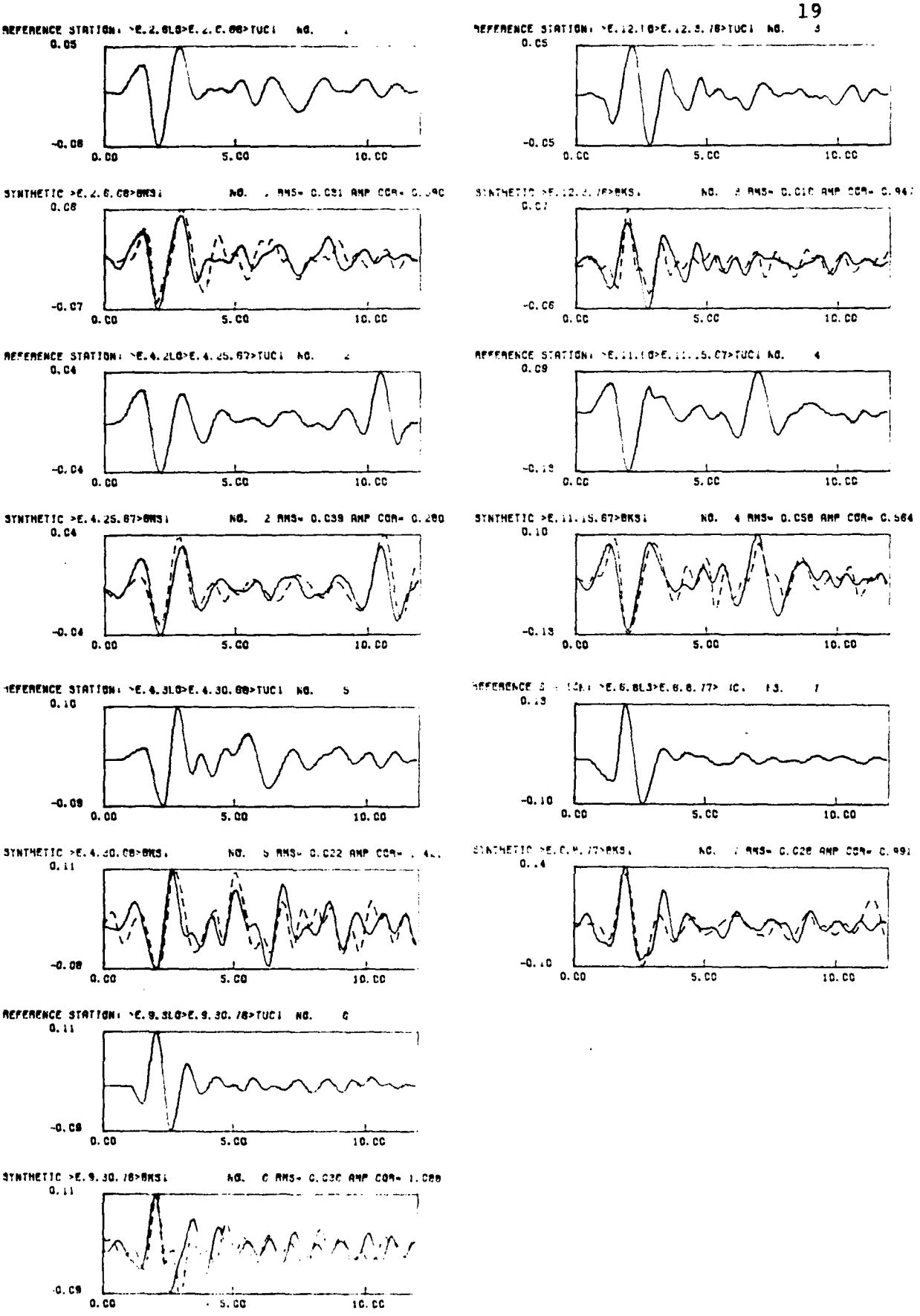

Figure 8. As Figure 7, but for BKS/TUC.

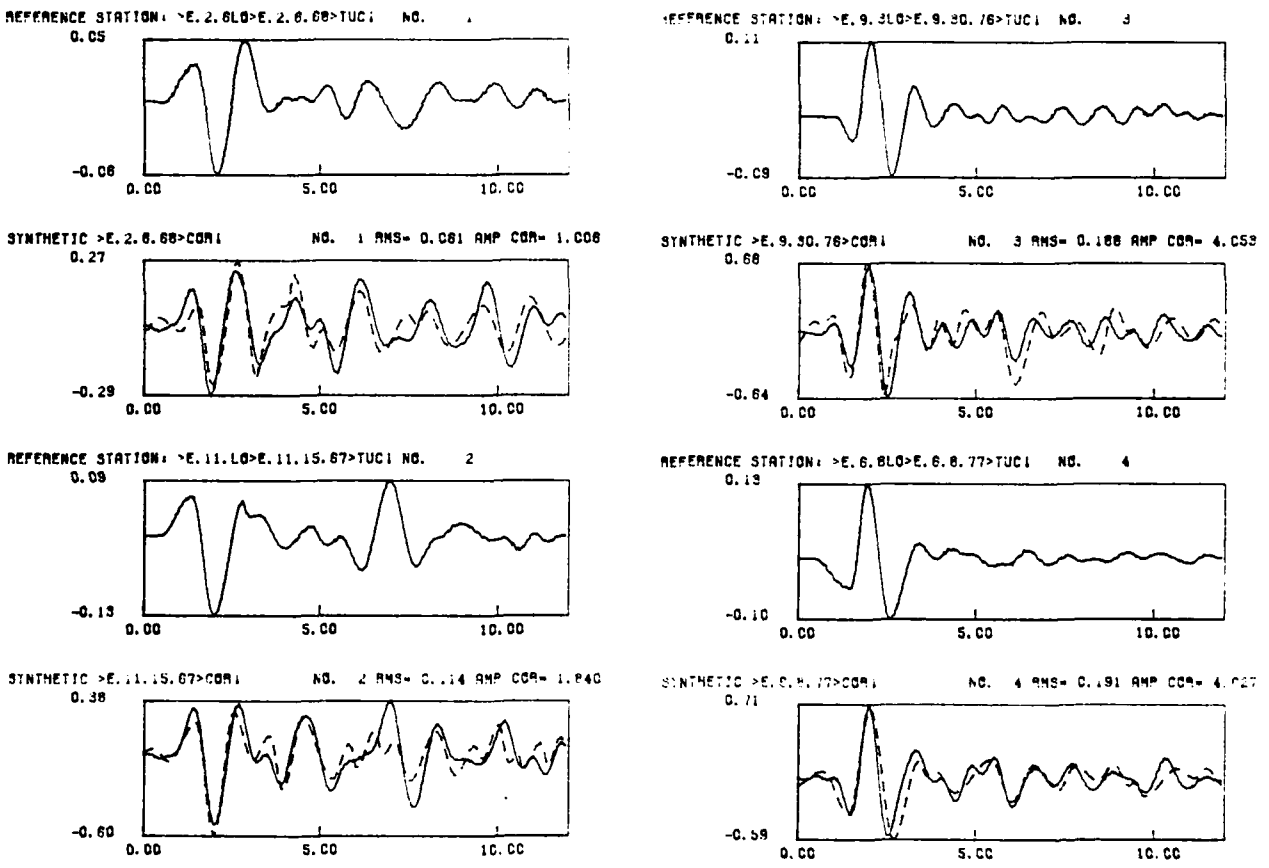

Figure 9. As Figure 7, but for COR/TUC.

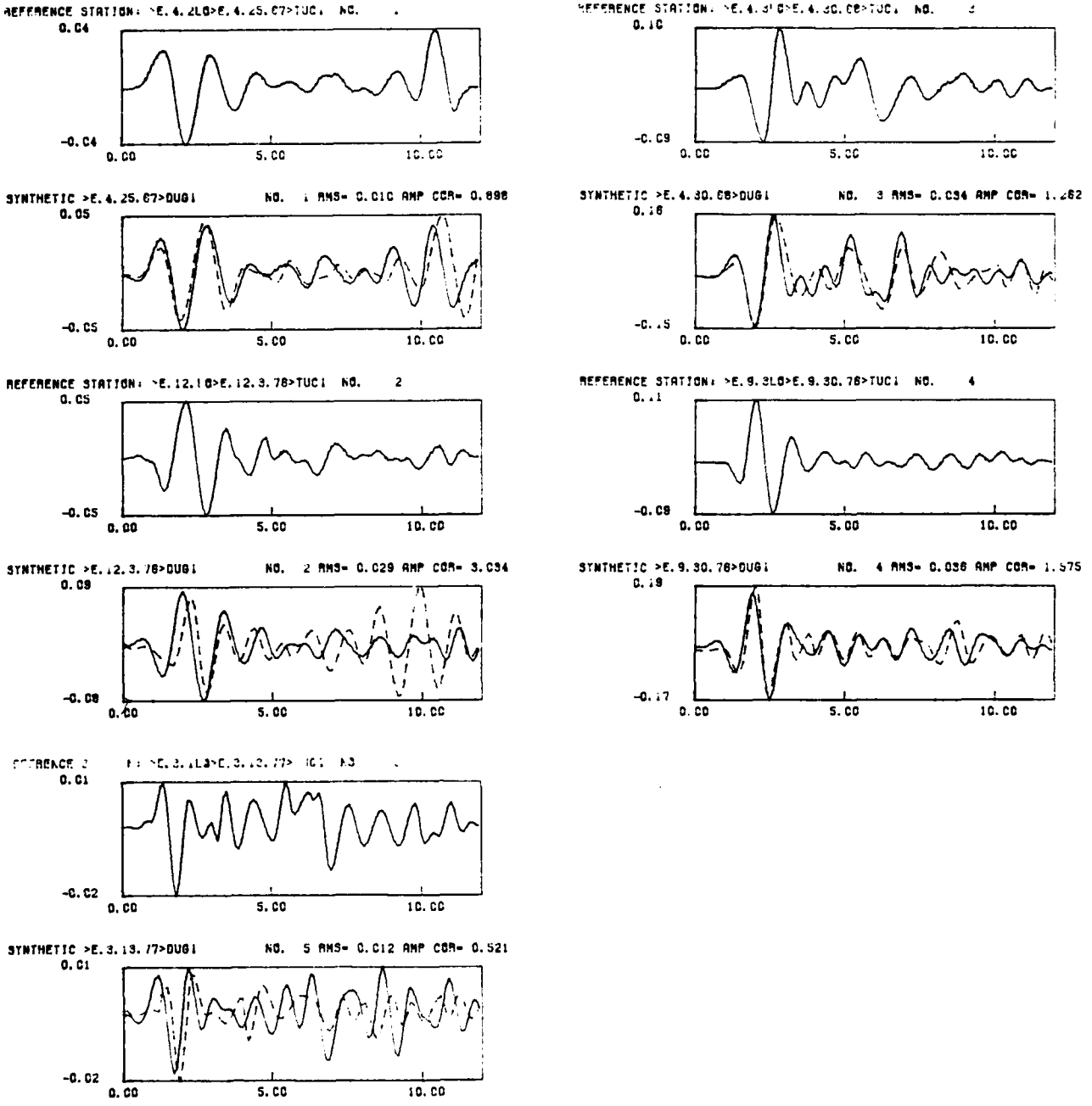

Figure 10. As Figure 7, but for DUG/TUC.

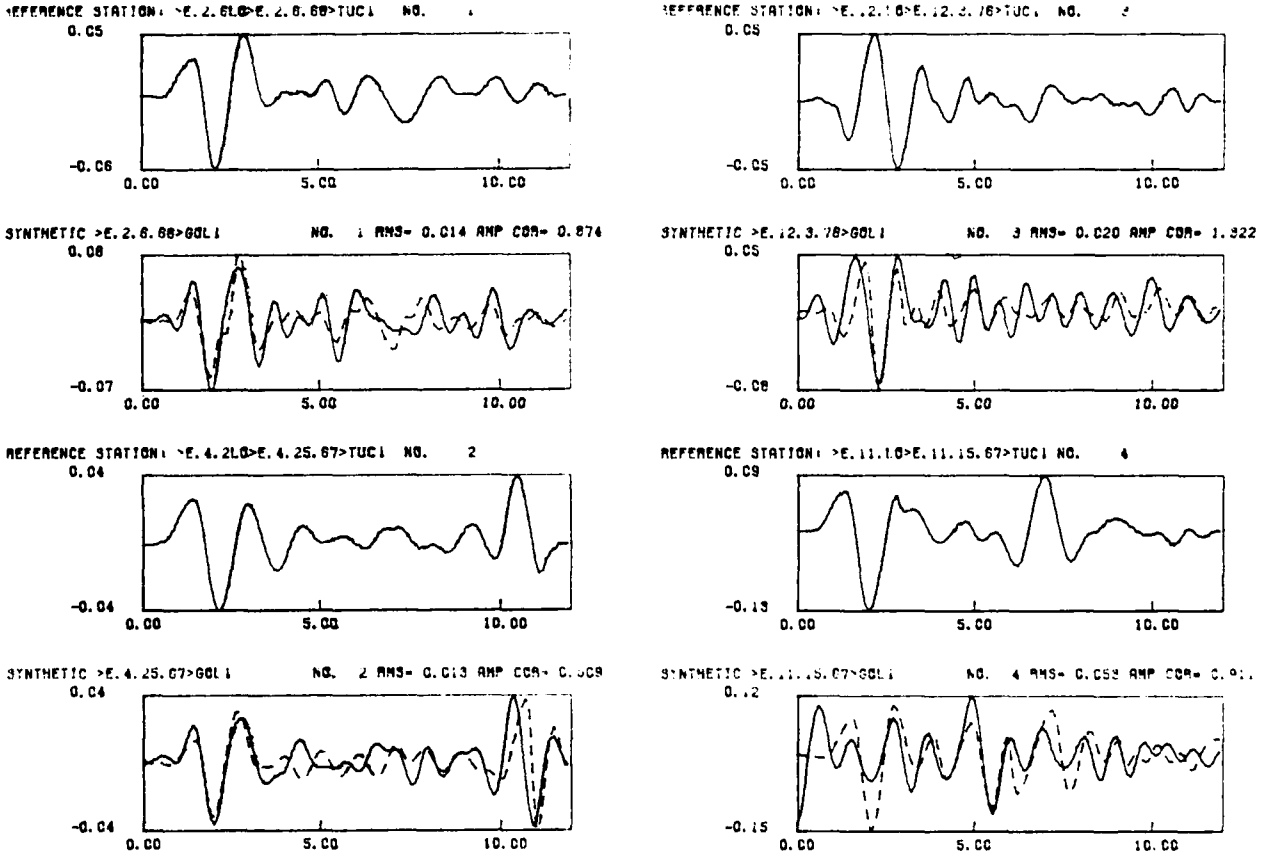

Figure 11. As Figure 7, but for GOL/TUC.

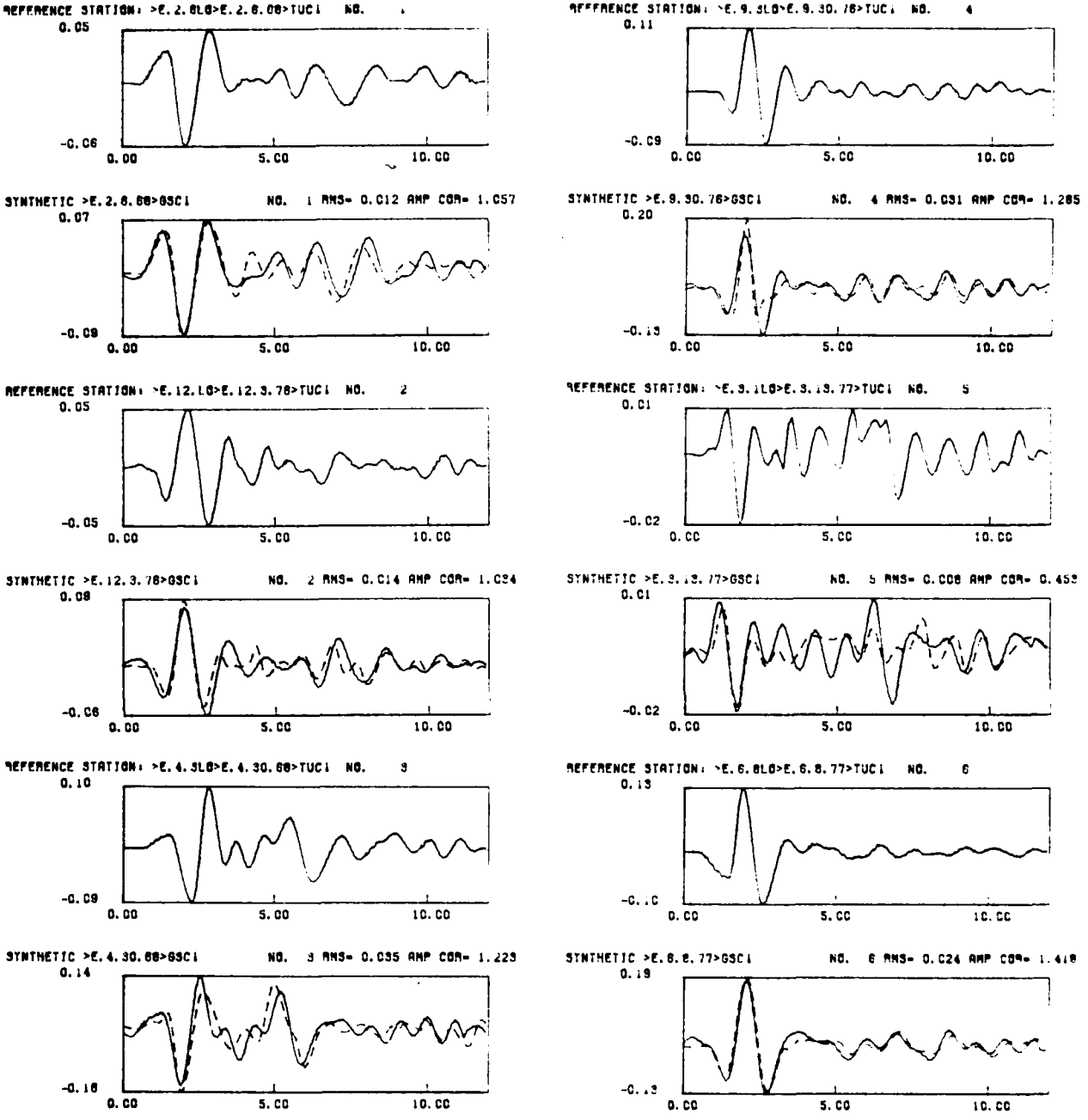

Figure 12. As Figure 7, but for GSC/TUC.

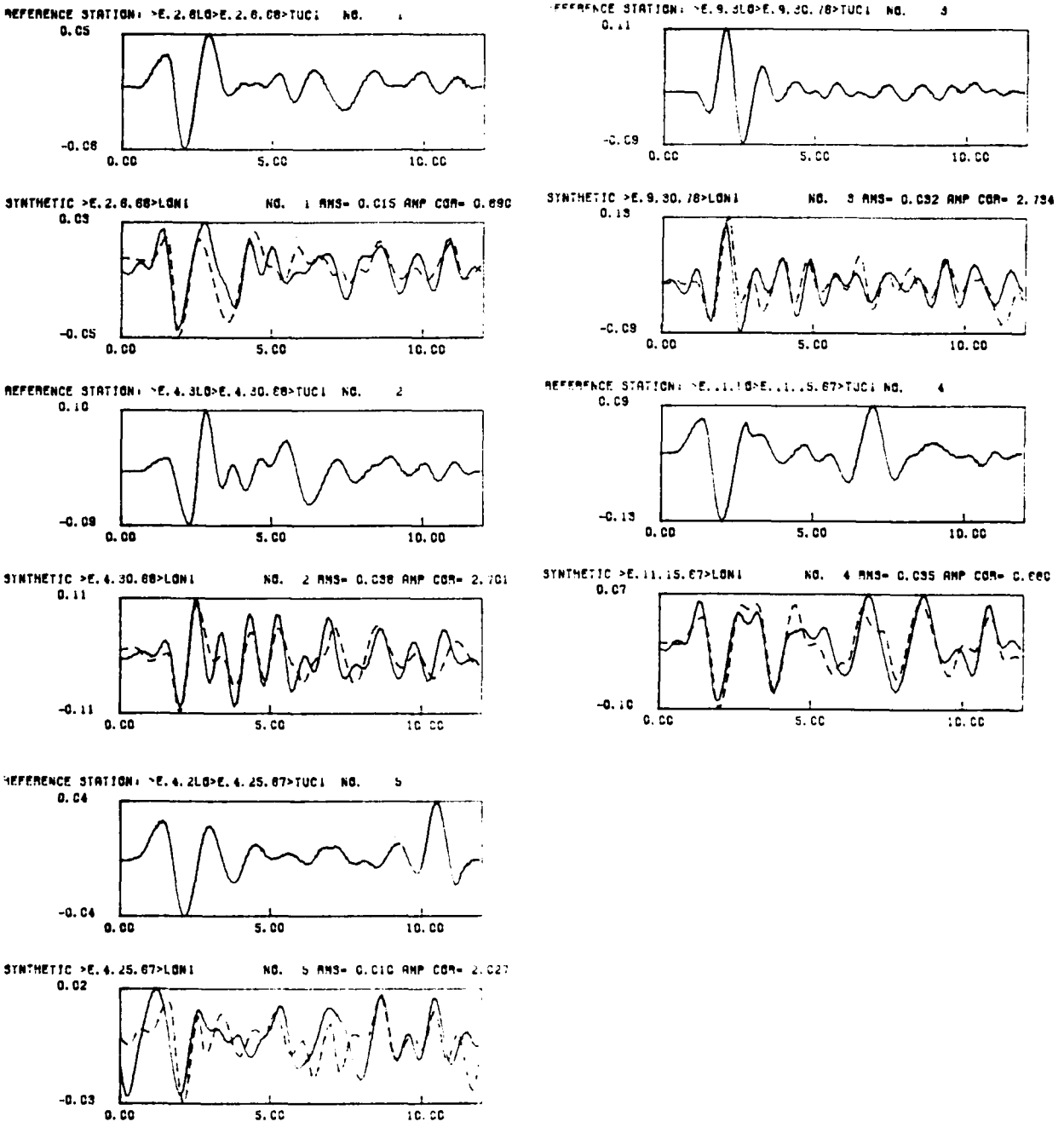

Figure 13. As Figure 7, but for LON/TUC.

and the secondary trace shown as the dashed line below. The solid line in the lower figure of each pair is the reconvolution of the reference trace with the frequency domain stacked deconvolution. In each case, a 6 second reference record was deconvolved from a 12 second secondary trace. Thus the resulting deconvolution operator will correctly predict only the first 6 seconds of the impulse response. The event of 12/3/76 in the deconvolution of DUG (Figure 10) shows what happens when an arrival exists on the secondary trace but not on the primary; while the event of 4/25/67 shows that the correct response is predicted if the reference station also receives the impulse. In spite of the problems always associated with hand-digitized data, the quality of the fits between observed and synthesized waveforms is quite respectable.

Figure 14 gives the estimated RRF's for two choices of reference station. The column on the left is referenced to TUC; while the column on the right is referenced to GSC. The changing of reference stations is accomplished simply by

$$d_i = \frac{r_i}{r_o} \cdot \frac{r_o}{r_j} = \frac{r_i}{r_j}$$

and the former reference station is handled by defining $d_o = r_o/r_o = 1.0$.

Though a glance at the two estimates of RRF's shows apparently significant differences, a better comparison is done in the context of synthetic seismograms. Figure 15 gives such a comparison for synthetics of a shallow event with the third focal mechanism in Figure 1. A little study of Figure 15 shows more similarity

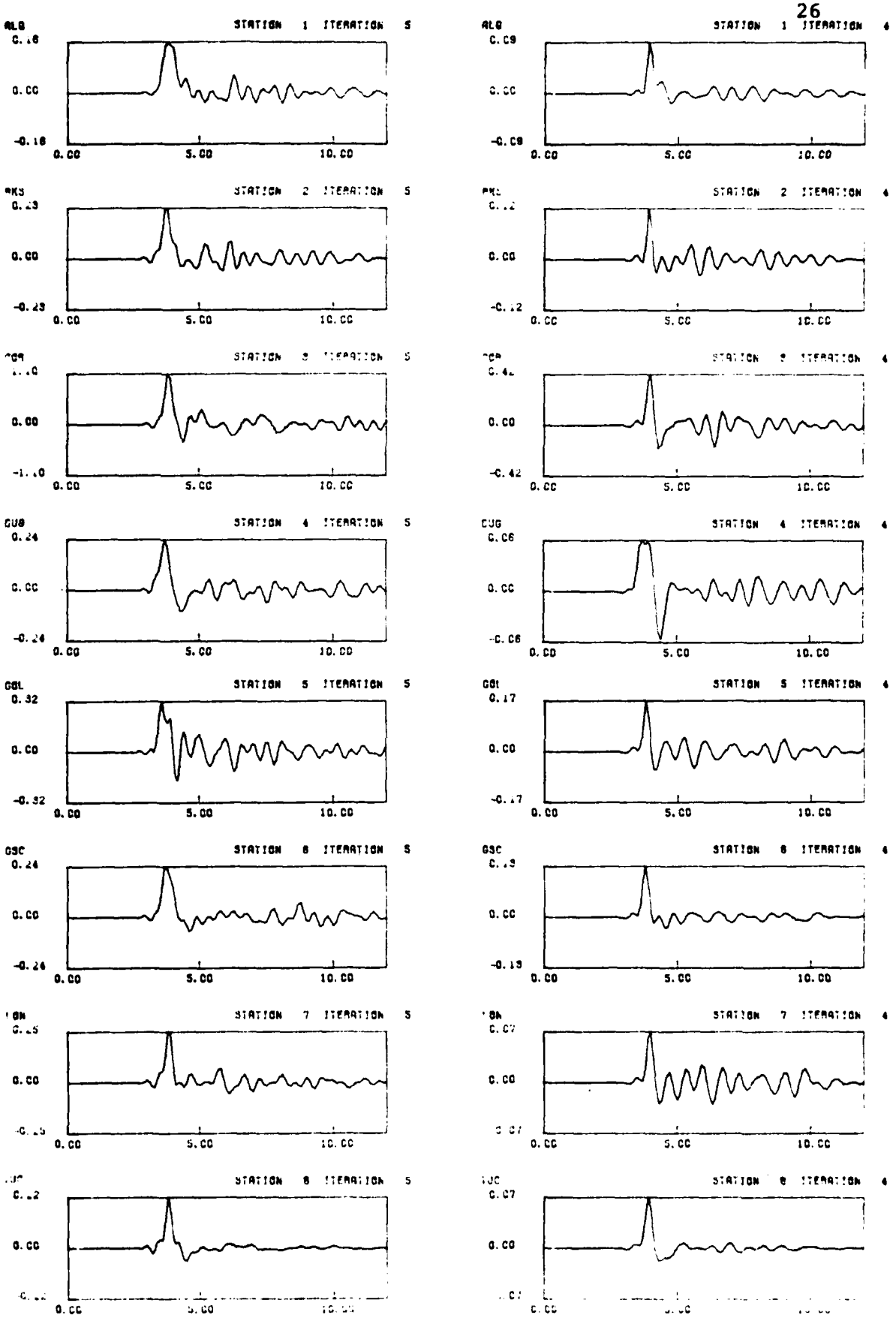

Figure 14. Estimated MED relative receiver functions appropriate for a southeast azimuth. Column at left referenced to TUC; at right referenced to GSC.

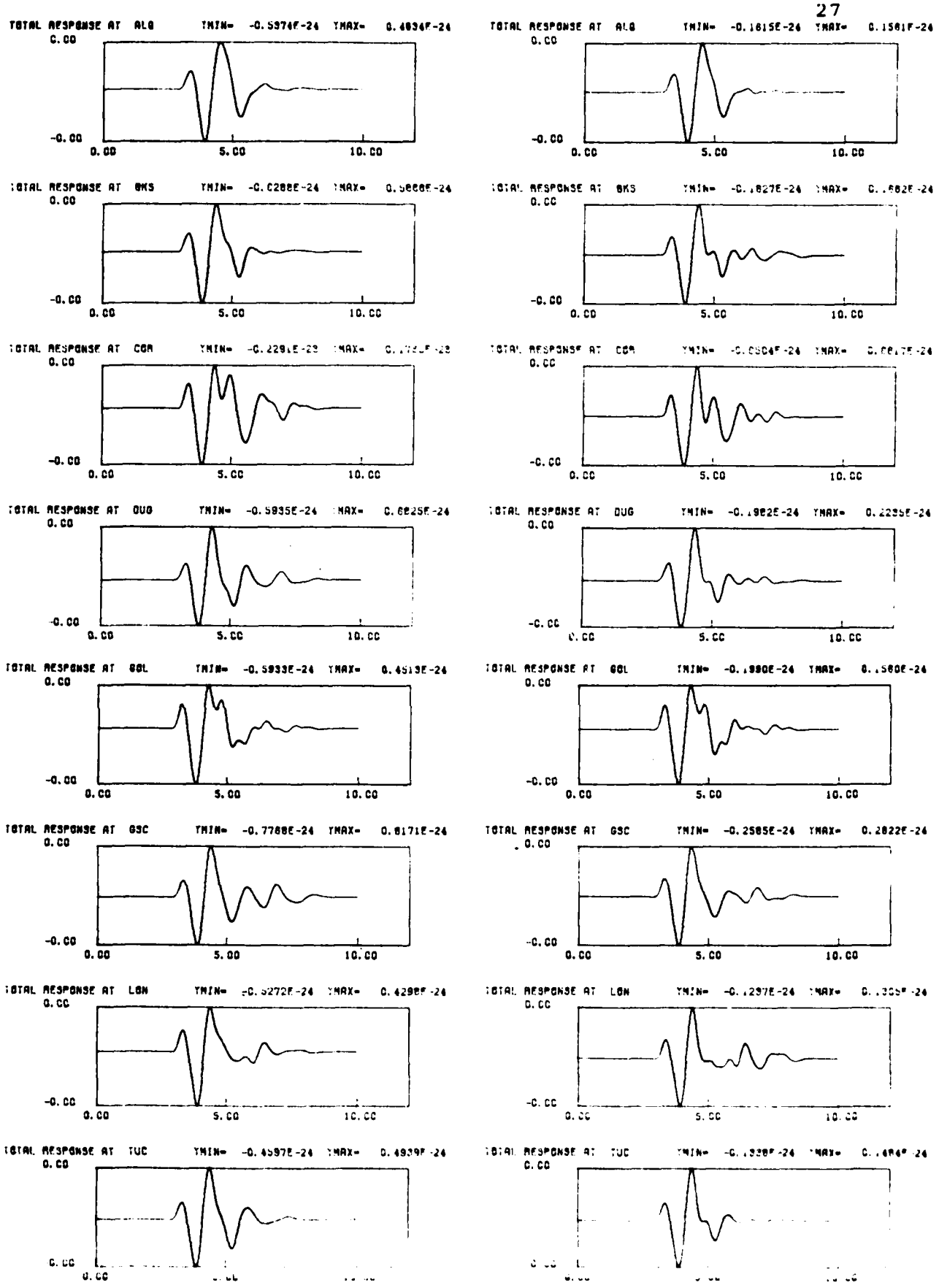

Figure 15. Synthetic seismograms computed by convolving the RRF's in Figure 14 with a simple earthquake source-time function.

as a function of recording station than as a function of referencing station. Clearly the two estimates of the RRF's are smoothed by convolution with the other propagation filters in such a way that the important information is nearly identical. This is an important confirmation that the MED process is converging to a stable and useful maximum.

The event list and data availability for events from the northwest azimuth are given in Table 2, and the data are given in Figures 16-21. Although 12 events were checked, usable data pairs are rare. Indeed, COR had to be excluded from this part of the study, and ALQ and LON were tentatively included with only 3 events each.

Figure 22 shows the MED estimated RRF's using station DUG for reference. The RRF's referenced to TUC were very similar, and gave nearly identical synthetic seismograms. The right hand column in Figure 22 shows the results of MED when the limited data stations ALQ and LON were excluded. Again, the two MED runs result in equivalent RRF's for the common stations in spite of the different starting configurations. The synthetic seismograms in Figure 23 confirm the stability of the estimated RRF's. Apparently the addition of two questionable stations to the MED data set does not degrade the results.

An interesting comparison may now be made between the RRF's in Figures 14 and 22 and between the synthetics in Figures 15 and 23. Some stations (ALQ and BKS) have very similar responses to arrivals from northwest and southeast azimuths; while others (GOL and GSC) have noticeably different responses. The arrival

TABLE 2. NORTHWEST AZIMUTH EVENT LIST

DATE	TIME	LOCATION	ALQ	BKS	DUG	GOL	GSC	LON	TUC
11/22/66	6:29:52	48.0N 146.8E			X	X	X	X	X
8/10/67	11:21:22	45.4N 150.3E	X	X	X	X		X	X
2/10/68	10:00:05	46.0N 152.3E	X	X	X	X	X	X	X
7/25/68	10:50:31	45.7N 146.7E		X	X				X
10/22/76	18:35:24	75.0N 134.9E	X						X
12/5/76	1:01:42	23.0N 140.0E			X		X		X
4/22/77	0:58:56	52.5N 138.8E		X		X			X
4/23/77	14:49:06	75.0N 134.9E			X				X
6/12/77	8:48:05	43.0N 142.3E			X		X		X

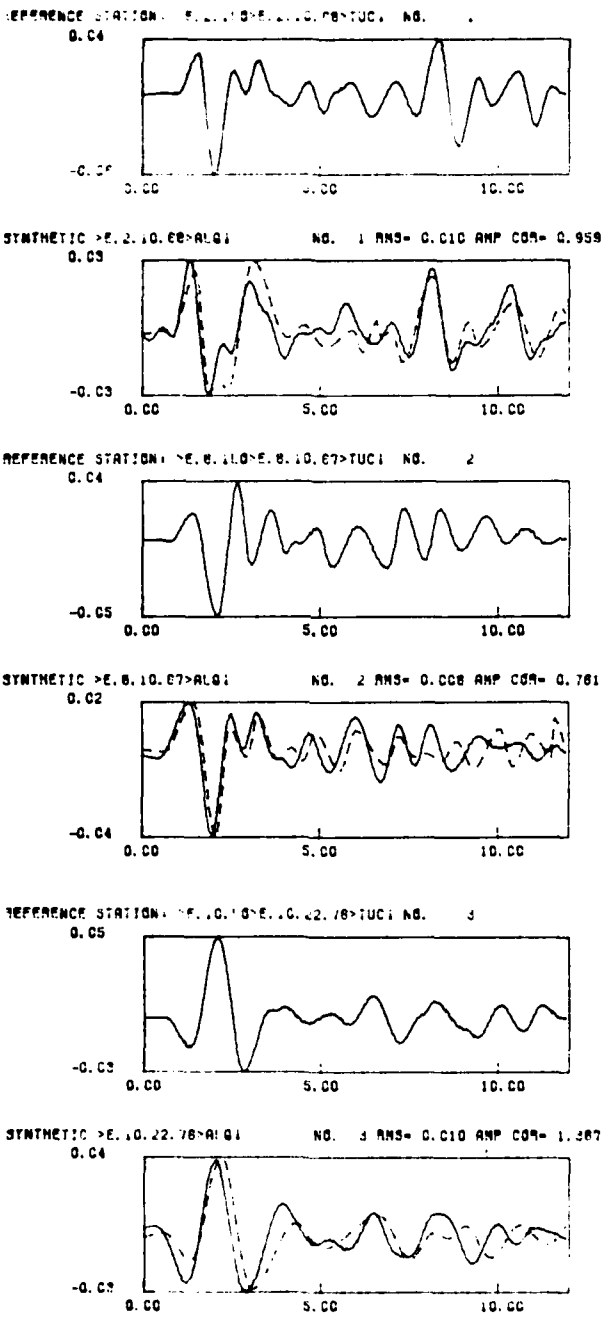

Figure 16. As Figure 7, but for ALQ/TUC at a northwest azimuth.

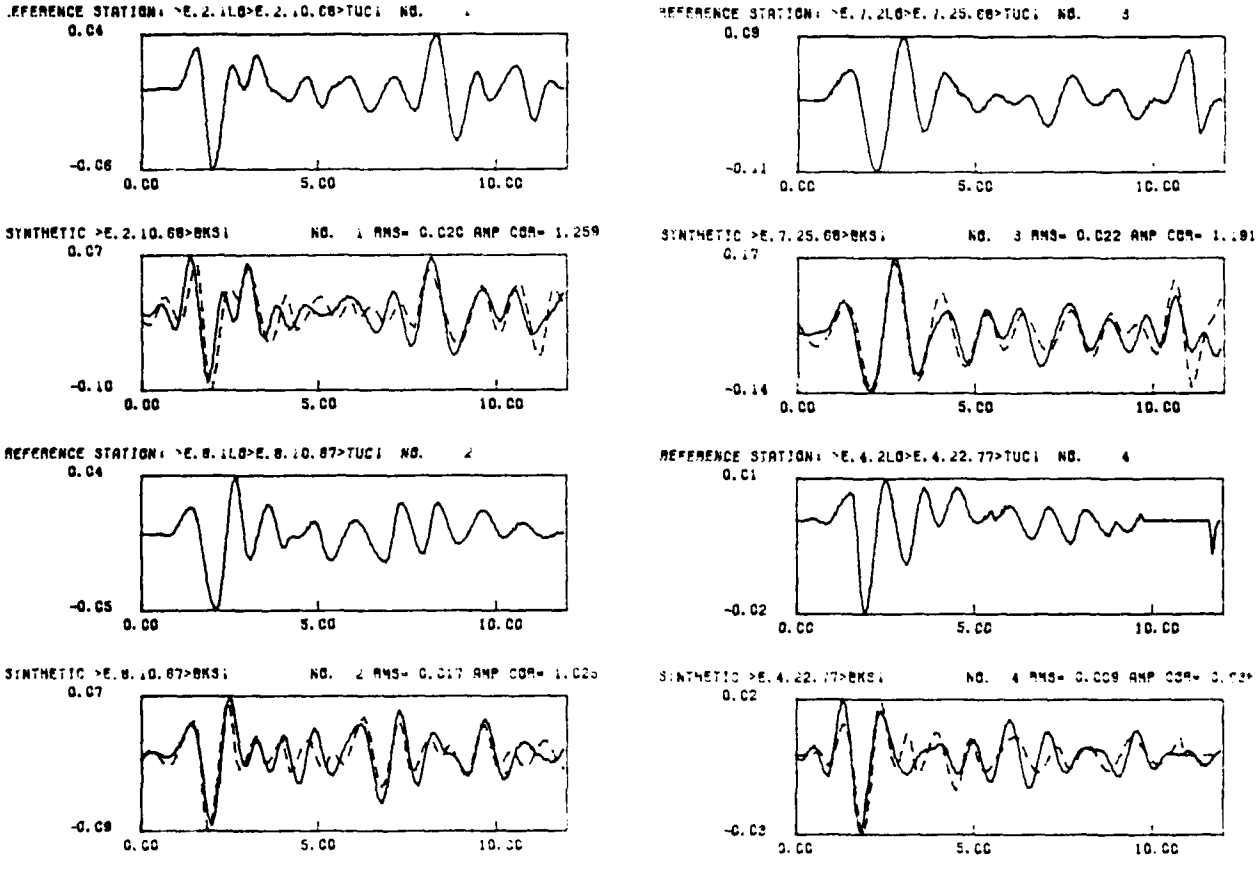

Figure 17. As Figure 7, but for BKS/TUC at a northwest azimuth.

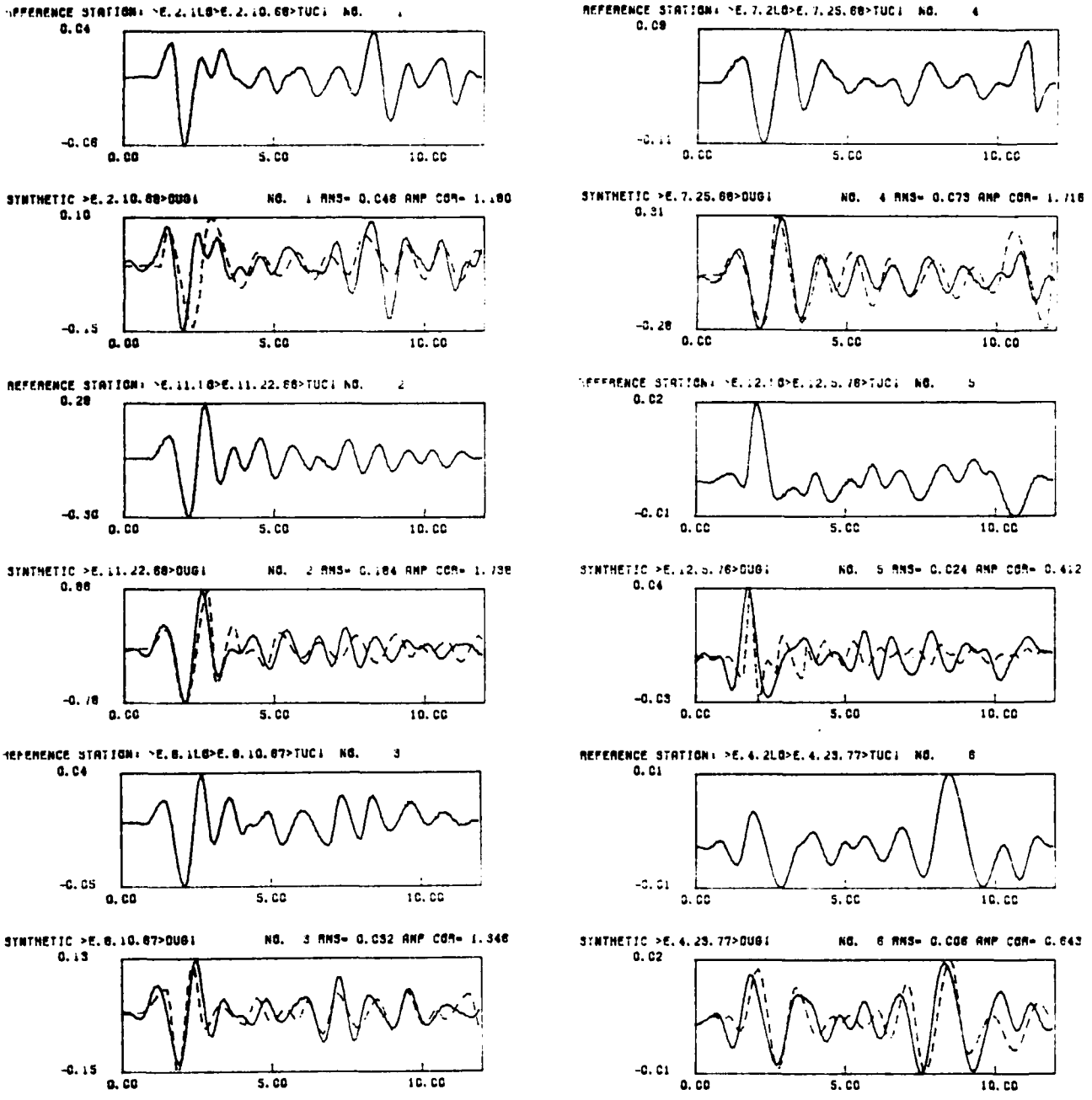

Figure 18. As Figure 10, but for DUG/TUC at a northwest azimuth.

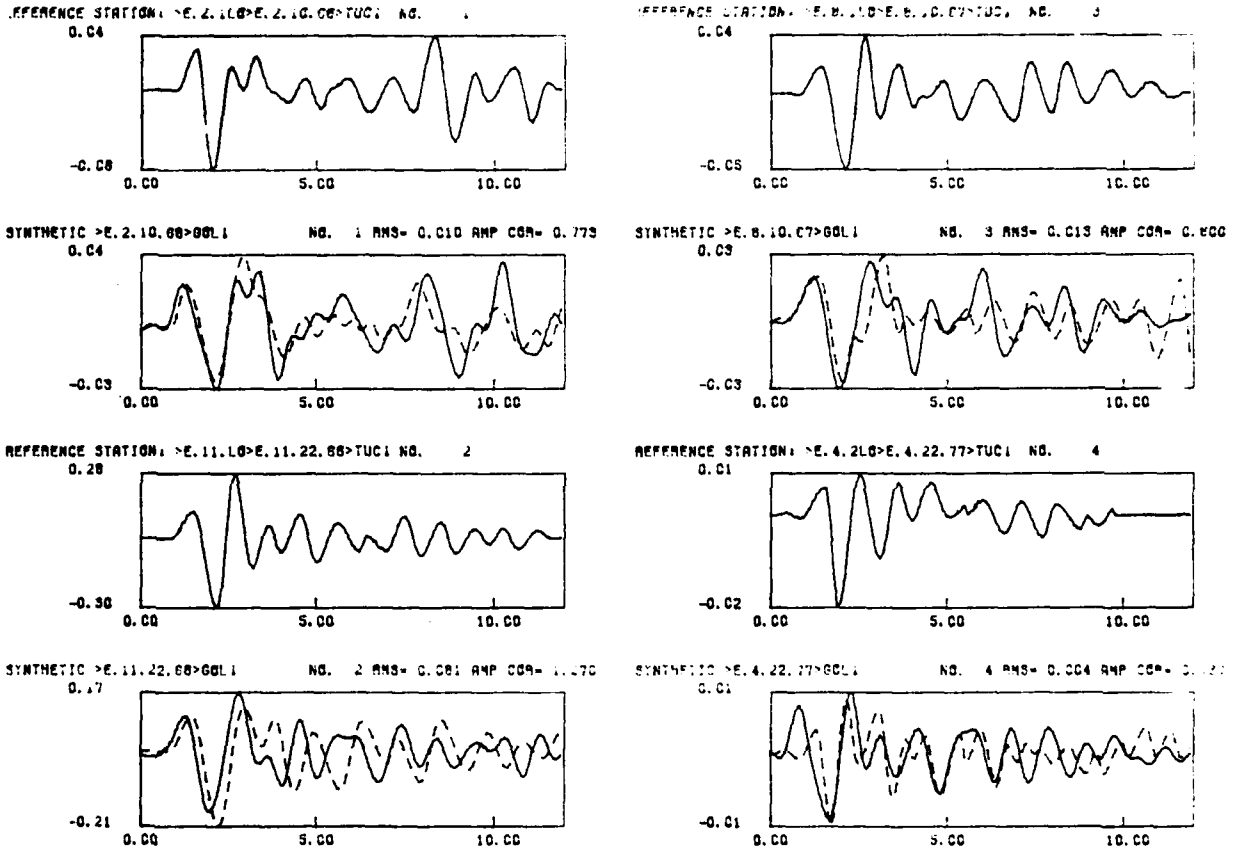

Figure 19. As Figure 11, but for GOL/TUC at a northwest azimuth.

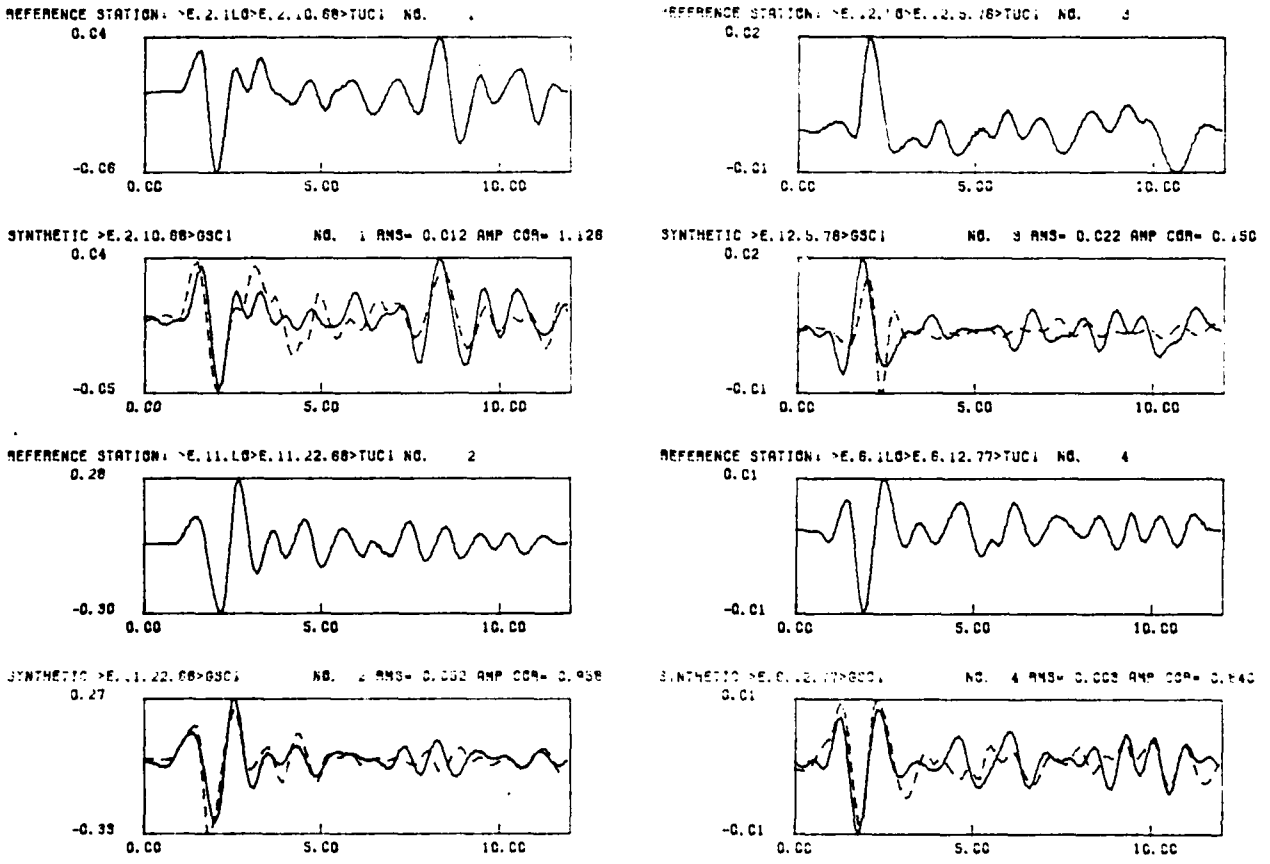

Figure 20. As Figure 12, but for GSC/TUC at a northwest azimuth.

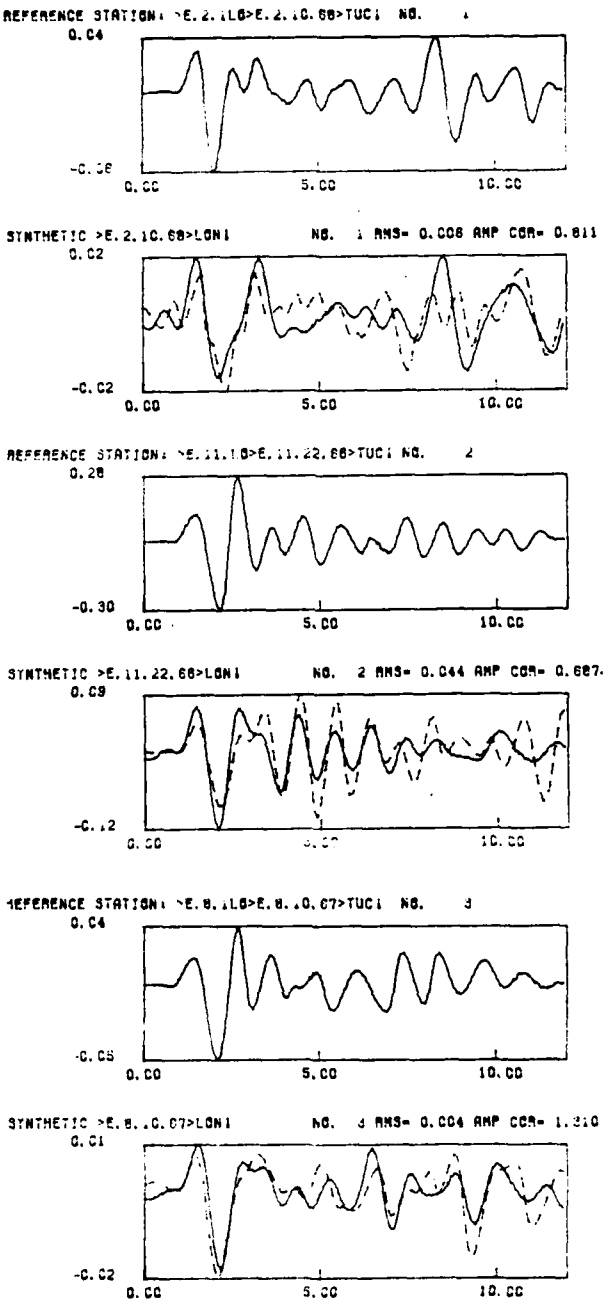

Figure 21. As Figure 13, but for LON/TUC at a northwest azimuth.

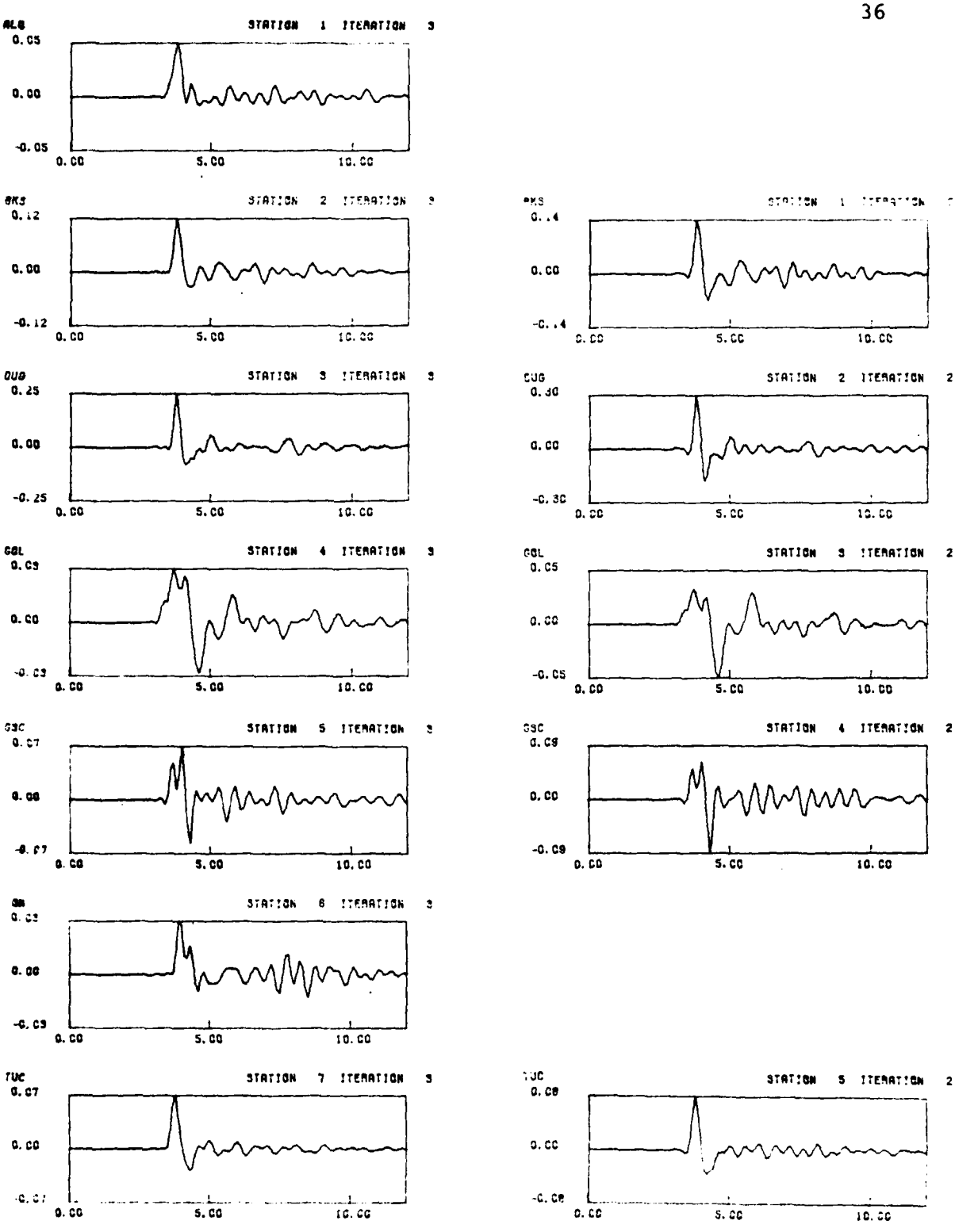

Figure 22. Estimated MED relative receiver functions appropriate for a northwest azimuth. The RRF's at the right were computed without stations ALQ and LON.

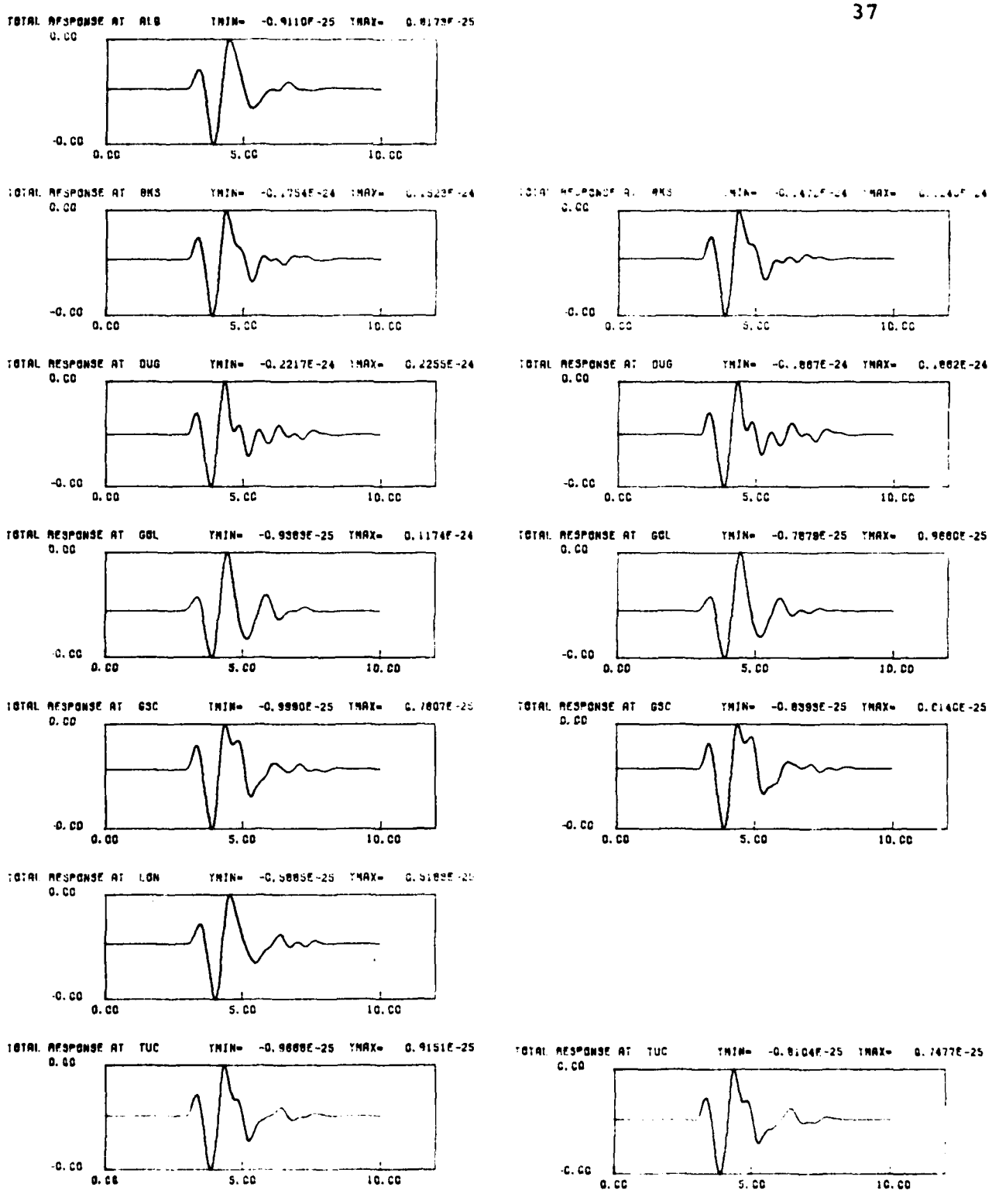

Figure 23. Synthetic seismograms computed by convolving the RRF's in Figure 22 with the same source-time function used for Figure 15.

at 3 seconds after P on the LON synthetics at both azimuths is a clear example of similar receiver function response predicted by entirely independent data sets. With enough data from enough azimuths, RRF's could be used to interpret crustal structure.

2.3.3 Eastern Kazakh Global Array

A receiver function study has been started for a global array about the Eastern Kazakh test site in the Soviet Union. Table 3 shows the data currently available at SGI for SRO, ASRO and several arrays in the distance range 30 - 95° about 21 presumed nuclear explosions. In spite of the number of events and the number of stations, very few useable trace pairs are available for deconvolution.

Based upon frequency content, CHTO was chosen for the reference station. Figure 2, in which t_1 is CHTO and t_2 is CTAO, demonstrates the problems involved with using a low frequency reference station. Figures 25 - 27 show the only possible deconvolutions with this SRO data set using CTAO as reference. Note that the waveforms at the four stations involved are very consistent, suggesting that it may be possible to generate additional CHTO reference traces by reconvolution of observed ANMO or CTAO traces with the inverse of the CHTO referenced deconvolution. This possibility will be examined during the next few months.

It should be noted that ANMO, CTAO and NWAO are at 95°, 92° and 90°, respectively, from the source region, and that their P body waves penetrate to within 100 to 150 km of the core mantle boundary. If a low Q zone exists there, as modeled by Anderson and Hart (1978), then a δt^* not associated with upper

TABLE 3. KAZAKH EVENT LIST

DATE	ANMO (95)	ANTO (33)	BCAO (68)	CHTO (35)	CTAO (92)	GRFO (42)	GUMO (64)	KONO (38)	MAJO (44)	NWAO (90)	TATO (41)	ATTU (39)	ALK (61)	KSRS (37)	LAO (84)	NAO (38)
3/20/76														22	13	
11/23/76	X				X					X						
12/7/76	X				X					X						
3/29/77					X									22	13	X
5/29/77	X									X						
7/30/77				X					X				4	20		
8/17/77													6		12	X
9/5/77	X			X	X									17		
11/30/77	X			X	X											
12/26/77												X	8		10	X
3/19/78				X									5	17	1	
6/11/78	X				X				X			X	4		13	X
7/5/78	X			X	X				X							
7/28/78	X				X					X		X	6	22		
8/29/78	X			X						X		X	4	18		
9/15/78	X	X			X			X	X							
11/4/78	X	X		X				X	X							
11/29/78	X	X		X		X			X							
6/23/79	X			X	X			X	X							
7/7/79	X	X				X		X	X	X						
8/4/79	X	X			X	X				X						

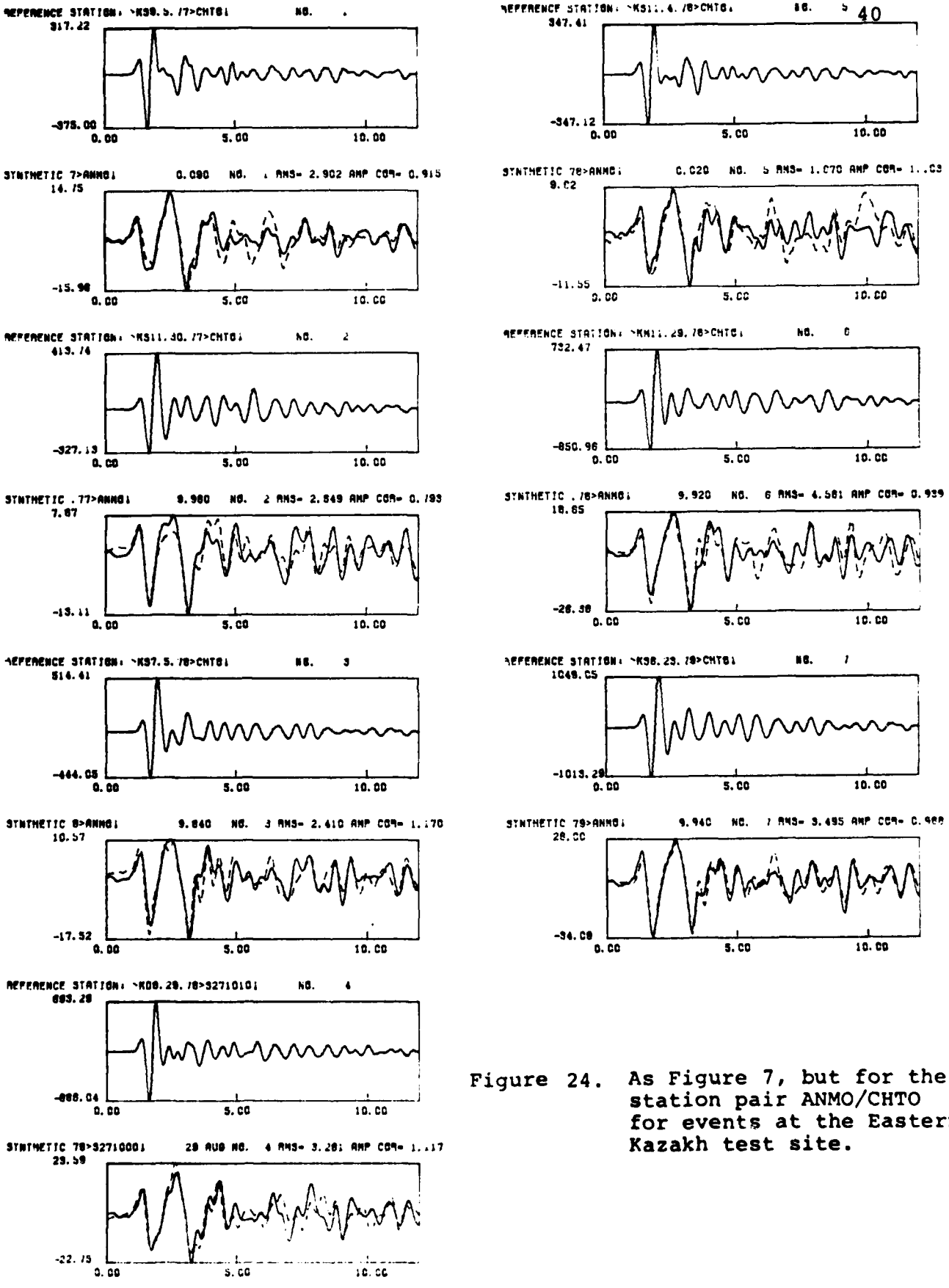

Figure 24. As Figure 7, but for the station pair ANMO/CHTO for events at the Eastern Kazakh test site.

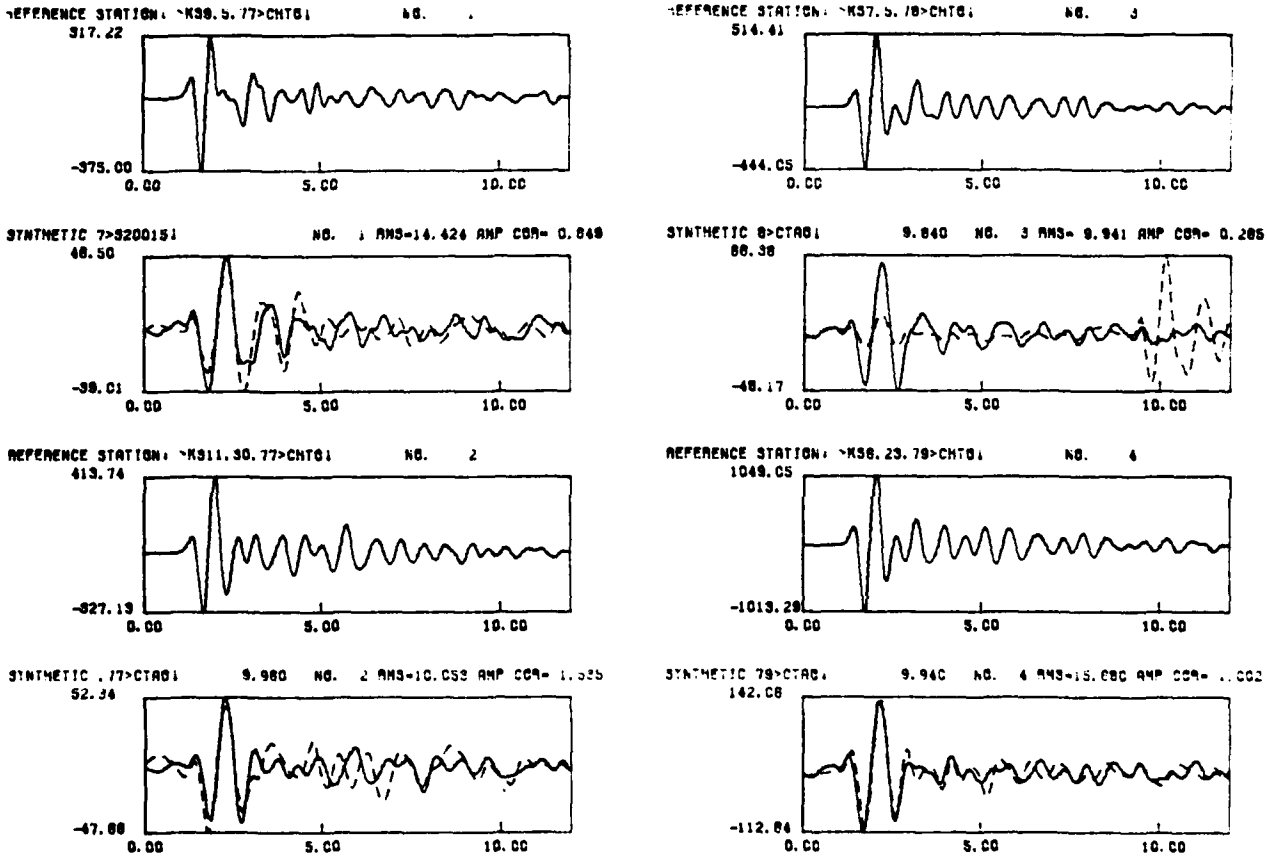

Figure 25. As Figure 24, but for the station pair CTAO/CHTO.

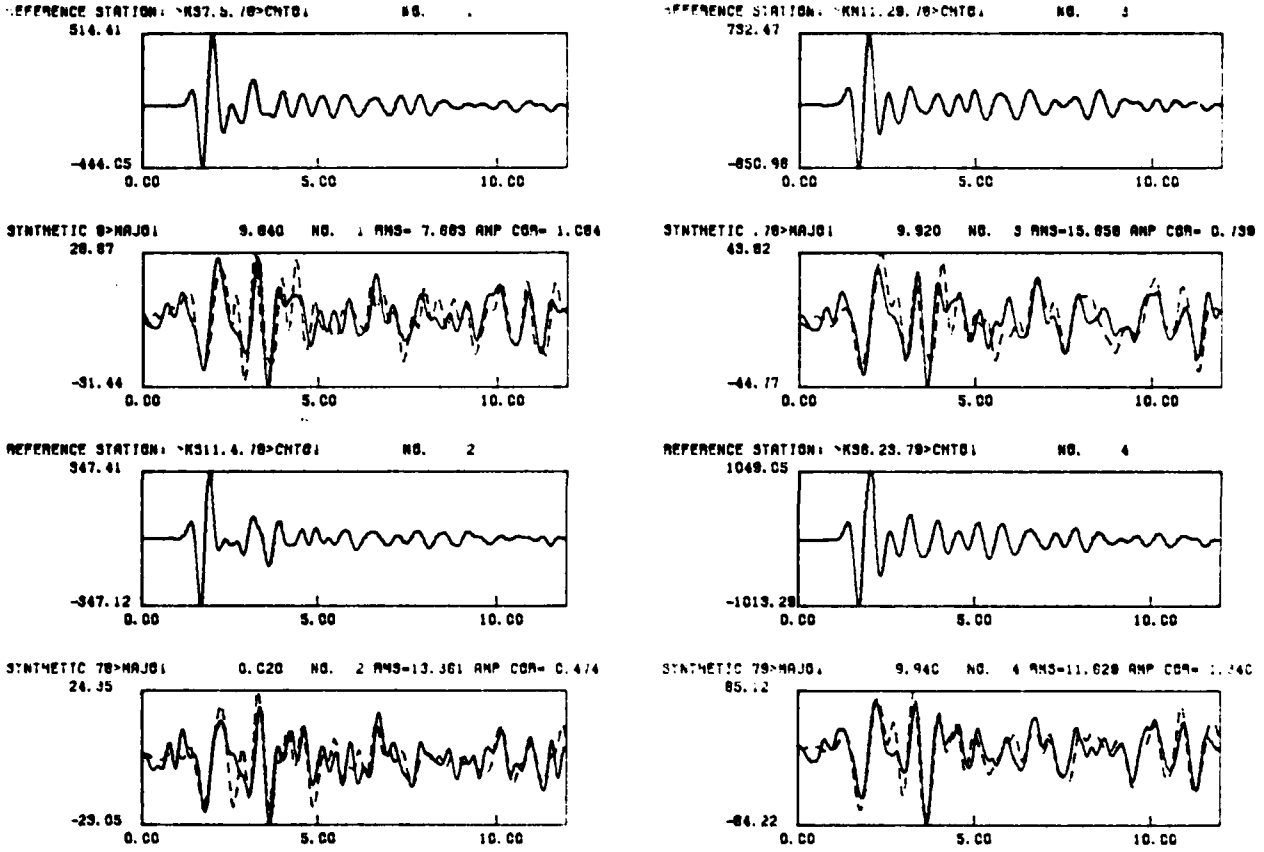

Figure 26. As Figure 24, but for the station pair MAJO/CHTO.

mantle behavior will be included in receiver functions computed with data from these stations. In some applications, such as predicting CHTO seismograms from ANMO data, this presents only the technical difficulty of working with inverse Q filters. The extra δt^* term does mean, however, that RRF's for ALQ (northwest azimuth) and ANMO (Eastern Kazakh) will not necessarily be comparable, and that the WUSA array cannot be tied to the Eastern Kazakh Global Array by this means.

MED outputs are not shown at this time for the global array; because of the lack of data. The data base is currently being expanded to enable both deconvolutions of the smaller arrays (KSRS, etc.) and the tying of these arrays into the global array.

III. CONCLUSIONS

The validity and practical applicability of the relative receiver function concept has been demonstrated for three types of arrays: the small array typified by the YF array at NTS; the continental array tested on the western United States, and the global array including all stations in a useable distance range about a given source region. In each case, reconvolutions proved that the average transfer functions can accurately predict seismogram behavior at one station based upon observed motion at another.

Several tests of the Maximum Entropy Deconvolution method have shown that it does produce stable and useful relative receiver functions. The method converges to the same practical result for different choices of reference station and for different

starting configurations, including different numbers of stations.

Much work remains to be done, especially with regard to tying together the different array concepts. In particular, if sufficient trace pairs can be developed between small arrays, such as KSRS and NORSAR, and the SRO network, then relative receiver functions within small arrays may be related to global networks.

IV. REFERENCES

Anderson, D. A. and R. S. Hart (1978). The anelasticity of the earth, J. Geophys. Res., 69, 2071-2084.

Hart, R. S., D. M. Hadley, G. R. Mellman and R. Butler (1979). Seismic amplitude and waveform research, SGI-R-79-012, Sierra Geophysics, Inc., Arcadia, California.

Lundquist, G. M. (1979). The Frequency Dependence of Q, Ph.D. Thesis, University of Colorado, Boulder, Colorado.

Mellman, G. R. and R. S. Hart (1980). Review of magnitude/yield estimation, Preliminary Report, SGI-R-80-017, Sierra Geophysics, Inc., Arcadia, California.

Wiggins, R. A. (1978). Minimum entropy deconvolution, Geoexploration, 16, 21-35.